


Gas Absorption Heat Pump #2 Performance Mapping

Project Number ET24SWG0003

GAS EMERGING TECHOLOGIES (GET) PROGRAM
January 2026

SoCalGas
Glad to be of service®

ICF

Prepared by ICF for submission to Southern California Gas Company

CONTENTS

LIST OF TABLES

LIST OF FIGURES

LIST OF EQUATIONS

Acknowledgements

ICF is responsible for this project. This project, ET24SWG0003, was developed as part of the Statewide Gas Emerging Technologies (GET) Program under the auspices of SoCalGas as the Statewide Lead Program Administrator. GTI Energy conducted experimental laboratory testing and provided technical guidance. Madeline Talebi provided project oversight with overall guidance and management from the ICF Technical Lead, Steven Long. For more information on this project, contact steven.long@icf.com.

Disclaimer

Executive Summary

The GET Program conducted a laboratory study to evaluate the performance of a commercially available gas absorption heat pump (GAHP) unit. In collaboration with GTI Energy, who provided laboratory services and technical assistance, a thorough test plan was developed to include equipment commissioning, a steady state evaluation, a defrost evaluation, and a load-based evaluation of the ANESI GAHP 80K unit.

During the steady state testing, the results proved to be consistent with the manufacturer's published data, therefore providing sufficient steady state capacity measurements to be implemented in the load-based analysis. Some troubleshooting of the system was needed as it was discovered that there was a partial system clog. The replacement of the filter-dryer before the expansion valve resolved the issue. Note that cycling behavior did occur when the unit operated at or near the GAHP's operating limits, but this is to be expected and does not correlate with the partial system clog.

Although the defrost testing proved to have minimal impact with an average derate of 1.0% relative to electric-driven heat pumps of up to 15%, it is recommended that additional defrost testing be conducted to properly characterize defrost derate across multiple operating conditions.

The load-based testing was conducted using the steady state testing operating conditions where various cycle ON and OFF times were tested under a standby losses test, a draw patterns test, and a low draw test. Based on the steady state capacity experimental data, the load-based curves were developed where the coefficient of performance (COP) as a function of part load percentage was modeled using a linear trendline across the three types of draw tests at approximately 90-100% of the GAHP unit COP over the part load range of 20-100%.

EnergyPlus modeling performance curves were developed, which resulted in a ±5% accuracy at full load and ±10% accuracy at lower part load ratios at all operating conditions evaluated according to the test plan developed.

Following an idle period, there was evidence of reduced performance and further clogging in a location that was not field replaceable. A replacement unit was installed at the end of October 2025, and load-based tests were repeated. It is believed that both the new control logic as well as eliminating possible clogging have resolved system performance issues.

Introduction

This study aims to characterize the steady-state and part-load (transient) performance of an ANESI GAHP 80K gas absorption heat pump (GAHP) unit with 100% natural gas (i.e., methane) to sufficiently populate model inputs in EnergyPlus. This study is a companion study to the completed Gas Emerging Technologies (GET) project – ET23SWG0015 GAHP Performance Mapping [1, 2]. Gas heat pump water technology is a newer technology where evidence-based lab testing has confirmed that the technology functions well and can save approximately 50% over the incumbent technology. Some key advantages of a GAHP unit over the incumbent equipment include the following [2, 3]:

- Reduction in energy usage – Heat pumps have the capability to operate over 100% efficiency (COP basis).
- Maintain optimal efficiency levels – The thermal "compressor" integrated in GAHP units is more efficient and has lower operation costs relative to traditional gas-fired appliances.
- Lower emissions – The reduction in fossil fuel consumption ultimately lowers emissions relative to traditional heating/cooling systems.
- Decentralized heating/cooling – GAHPs can be installed close to buildings or heating zones that they serve as opposed to relying on a central plant. This reduces the need for extensive energy transportation infrastructure.

With water heating being the largest non-industrial end-use of natural gas in California, a significant impact can be made where reductions in natural gas consumption are implemented. This study spans all sectors and all applications.

With the recent passing of California legislation including SB 1477 (building decarbonization/space heating/water heating), California Long-Term EE Strategic Plan (CLTEESP), and AB 758 (comprehensive energy efficiency in existing buildings law), there is a collective push for energy efficiency solutions specifically in the commercial sector.

The testing to support EnergyPlus modeling consists of both static performance mapping and transient performance mapping.

Assessment Objectives

The main objective of this laboratory study was to conduct a comprehensive analysis the ANESI GAHP 80K unit to integrate performance mapping curves in EnergyPlus. This is part of an ongoing study to test various market-ready heat pump units to contribute to the EnergyPlus heat pump modeling portfolio and increase its overall accuracy and versatility. Within the EnergyPlus modeling space, the primary objectives include forecasting of energy consumption, utility bills, and greenhouse gas (GHG) emissions. The target audience includes California policymakers, program designers, software developers, and manufacturers.

Test Plan

The test plan was designed to split the laboratory testing into three phases – commissioning, steady state evaluation, and load-based (transient) evaluation. The commissioning phase of the system was based on the manufacturer's published performance data per the test point outlined in Table 1. Corresponding testing tolerances for the commissioning phase are outlined in Table 2.

Table 1: Target Conditions for Commissioning Test.

Test Point	Dry Bulb Outdoor Air Temperature (OAT), °F	Return Temperature (RT), °F	Flow Rate, GPM
1	47	95	8.3

Table 2: Commissioning Test Tolerances.

Variable	Tolerance
Return and Supply Heating Loop Temperatures	±1.0°F
Heating Loop Flow	±2.0%
Simulated Outdoor Air Dry-bulb Temperature	±1.0°F
Firing Rate	±2.0%
ANESI GAHP 80K Electrical Power	±1%
% O_2, % CO_2 in Exhaust (Initial Commissioning Only)	±0.4%

The steady state evaluation was performed over a range of operating conditions outlined in Table 3. In addition to a steady state evaluation, Table 4 outlines the test points for the defrost evaluation. Corresponding testing tolerances for the steady state phase are outlined in Table 5.

Table 3: Target Conditions for Steady State Evaluation.

Test Point	Dry Bulb OAT, °F	Firing Rate, kBtu/h	RT, °F	Firing Rate, kBtu/h	RT, °F	Firing Rate, kBtu/h	RT, °F
1-12	110	55 (94% = Max)	1) 95 2) 110 3) 120 4) 130 (Max)	28 (50%)	1) 95 2) 110 3) 120 4) 130 (Max)	14 (25% = Min)	1) 95 2) 110 3) 120 4) 140 (Max)
13-24	90						
25-36	75						
37-48	60						
49-60	47						
61-72	35						
73-84	17						
85-96	7						
97-108	0*						
* = or minimum chamber temperature							

Table 4: Target Conditions for Defrost Evaluation.

Test Point	Dry Bulb OAT, °F	Firing Rate, kBtu/h	RT, °F
1	40	55	110
2	30		
3	20		

Table 5: Steady State and Defrost Evaluation Tolerances.

Variable	Tolerance
Return and Supply Heating Loop Temperatures	±2.0°F
Heating Loop Flow	±2.0%
Simulated Outdoor Air Dry-bulb Temperature	±2.0°F
Glycol Concentration	±3.0%

The ANESI GAHP 80K was designed to modulate the supply temperature (ST) of the glycol by firing from 100% to 25% of the design capacity. The control function is as follows:

- When the tank is cold, ST is below the controller setpoint. The controller will fire the unit at 100% capacity.
- As the tank heats up, both ST and return temperature (RT) will increase. When the ST approaches the setpoint, the controller modulates the combustion firing rate using

proportional-integral-derivative (PID) control logic. Firing rate modulates from 100% to 25% to maintain ST.

- If there is minimal water draw, the ST reaches the control setting and reduce firing capacity to the minimum. If tank temperature continues to rise, the aquastat temperature is satisfied and shuts off the unit.
- When water draw commences, the tank temperature drops and the aquastat sends a call for heating. The unit begins firing to achieve the ST setpoint.
- The aquastat, located at the midpoint of the tank, functions as the water temperature control.

Therefore, due to the nature of the ANESI GAHP 80K unit, the load-based evaluation was performed over a range of operating conditions. Table 6 outlines the Standby Losses test which measured tank losses under a no-draw condition at two tank temperatures. The system was operated through the longer of three on/off cycles. While the tank under most conditions was placed indoors and less affected by ambient conditions, the system performance was tested at high (90°F), moderate (47°F), and low (17°F) temperatures.

Table 6: Target Conditions for Load-Based Evaluation – Standby Losses.

Dry Bulb OAT, °F	Tank Setpoint, °F
90	1) 120 2) 140
47	
17	

Table 7 outlines the Low-Draw test which was performed by testing steady-state flows of 12 and 24 gallons per hour (approximately 10% and 20% of the unit rated capacity). Therefore, the unit will cycle to its lowest firing rate and then cycle off. The system was operated through three on/off cycles. Operational characteristics and performance of the unit were monitored.

Table 7: Target Conditions for Load-Based Evaluation – Low-Draw Testing.

Dry Bulb OAT, °F	Draw Rate, gph	Aquastat Setpoint, °F	City Water Temp, °F
90	12 24	120 140	60, 80
47 17	12 24	120 140	60

Draw pattern testing was based on the load profile developed from test modeling of multi-family buildings done by the Ecotope tool [3]. This draw pattern was used with draws of

1,000, 3,000, and 5,000 gallons per day (gpd) as shown in Figure 1. The test matrix associated with the proposed draw pattern is shown in Table 8.

Figure 1: Proposed Draw Patterns for Load-Based Testing. Values are shown for 3,000 gpd.

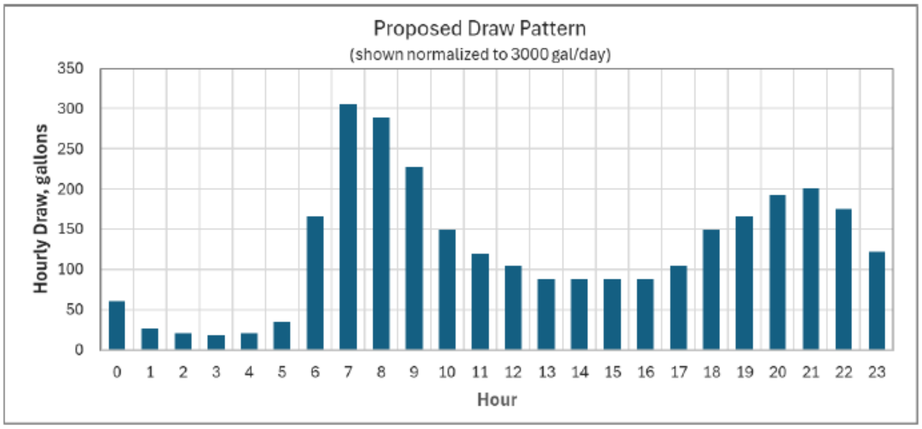

Table 8: Target Conditions for Load-Based Evaluation – Draw Pattern Testing.

Dry Bulb OAT, °F	Daily Draw (gallons)	Aquastat Setpoint, °F	City Water Temp, °F
47	1,000 3,000 5,000	120 140	60

Corresponding testing tolerances for the load-based evaluation are outlined in Table 9.

Table 9: Load-Based Tolerances.

Variable	Tolerance
Return and Supply Heating Loop Temperatures	±5.0°F
Heating Loop Flow	±2.0%
Simulated Outdoor Air Dry-bulb Temperature	±5.0°F
Glycol Concentration	±3.0%

Equipment Commissioning

The ANESI GAHP 80K commercial water heater was installed in GTI Energy's thermal heat pump (THP) testbed. Figure 2 shows the installation from multiple angles.

Figure 2: GAHP Installation Pictures.

Figure 3 shows the measuring and verification (M&V) instrumentation used for this evaluation, including the THP testbed environmental chamber equipment. Simplified details and tags of the M&V instrumentation are described in Table 10.

Figure 3: Diagram of the M&V Instrumentation and THP Testbed.

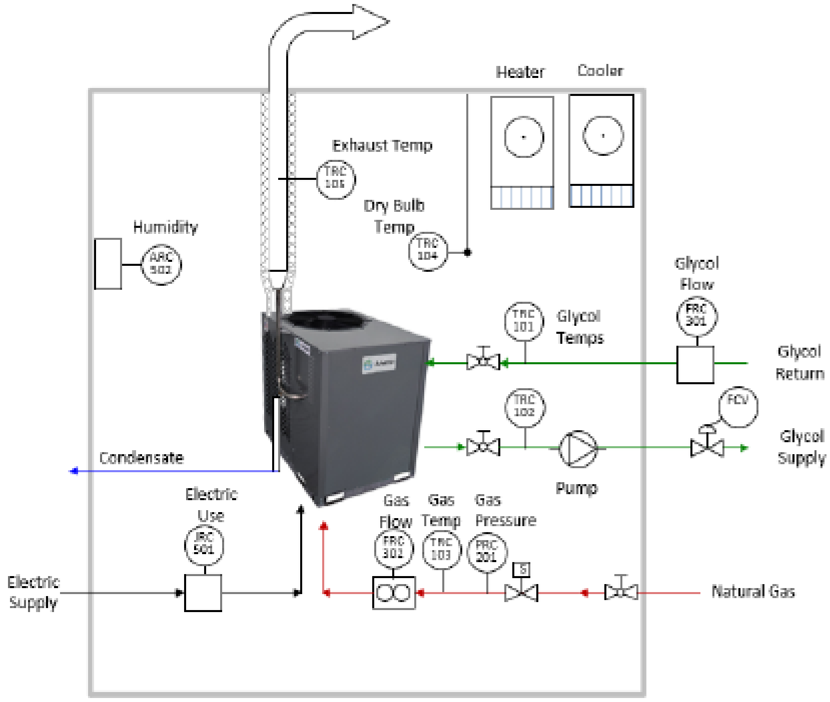

Table 10: Instrumentation Tags and Details.

Instrumentation Tag	Measurement
RTD1	GAHP return temperature
RTD5	GAHP supply temperature
TC15	Natural gas temperature
TC12, 13, and 14	Environmental chamber temperatures
TC11	Exhaust gas temperature
NG PT	Natural gas inline pressure
FT1	GAHP flow rate
GM	Natural gas flow rate
EPT	GAHP power
RH1	Environmental chamber humidity

Additional details regarding the commissioning process and the test rig setup can be found in the Appendix 1.0 Test Rig Setup section.

The ANESI GAHP 80K system was operated under predefined steady-state rating conditions. Published ratings are at a hydronic return temperature of 95°F, ambient temperature of 47°F, and water flow rate of 8.5 gpm. At these conditions, the ANESI GAHP 80K's rated output is 78,000 Btu/h.

The commissioning was performed using the following procedures:

- The evaluation was conducted by running the ANESI GAHP 80K after verifying the gas exhaust constituents at 30% and 90% burner demand.
- A service technician bled non-condensables from ammonia-water solution until discharge head pressure was about 260 PSIG.
- The THP testbed equipment controlled the target simulated OAT and ANESI GAHP 80K hydronic ST.
- The evaluation took approximately 60 minutes to achieve the adequate operating conditions.
- Energy rates were calculated and compared with the manufacturer's specifications.

The time series of key data in the commissioning evaluation are show in Figure 4 with a nominal 94% burner firing rate until approximately 1:10 elapsed time, and then at 30% burner firing rate. The burner firing rate of 94% was found to match the rated firing rate, 54,500 Btu/h. Each burner firing was commissioned at 95°F target RT (0:36 to 1:10 elapsed time for 94% and 1:45 to 2:00 for 30%). The resulting 15-minute average parameters are listed in Table 11 at 94% burner demand and 95°F target RT.

Figure 4: Commissioning Time Series.

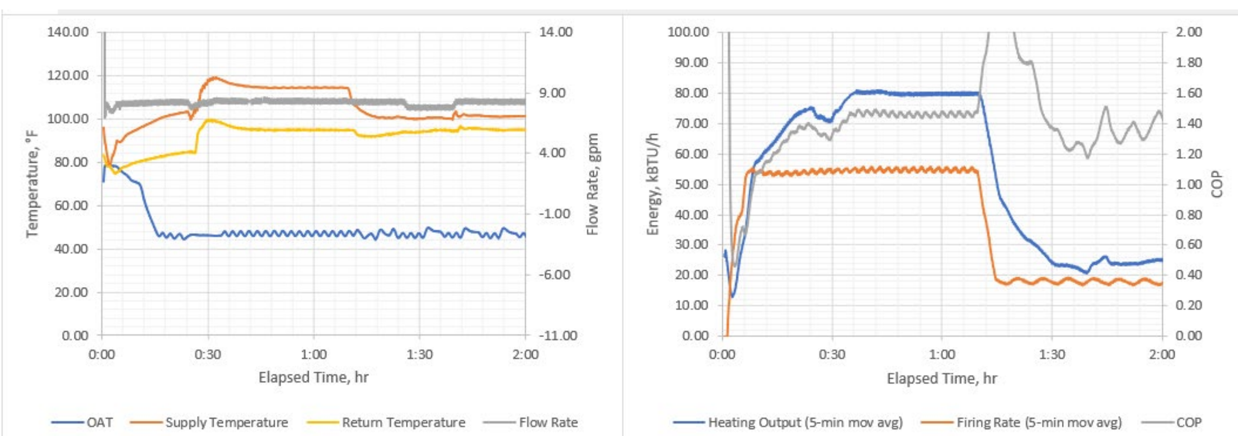

Table 11: Commissioning Test Results vs. Published Values.

Variables	Test Results	Published Values
Flow Rate	8.3 gpm	8.5 gpm
OAT	47.0°F	47.0°F
Return Temperature	95.0°F	95.0°F
Supply Temperature	114.4°F	113.5°F
HHV Used	1,050	1,020
Energy Output	79,860 Btu/h	78,000 Btu/h
Energy Input	54,800 Btu/h	54,500 Btu/h
NG Flow Rate	52.2 cfh	53.4 cfh
Gas COP	1.46	1.43

Calculations

Steady State and Load-Based Evaluation

The performance results include the energy input, power, heating output, and the COP. The energy input were calculated using Equation 1.

Equation 1: Energy Input.

$$Q_{in} = \sum V_g \cdot \frac{P_a}{P_s} \cdot \frac{T_s}{T_a} \cdot HHV$$

where

Q_{in} = accumulated natural gas energy input, British thermal unit (Btu)
V_g = natural gas volume, cubic foot (CF)
P_a = actual line pressure and barometric pressure, pounds per square inch absolute (psia) (referencing weather data)
P_s = standard pressure of 14.969 pounds per square inch (psi)
T_a = actual line temperature, °R
T_s = standard temperature of 520°R
HHV = natural gas higher heating value (HHV), Btu/cF (values were measured daily)

Following these calculations in Equation 1, the energy input is converted to a firing rate as a rolling average over each test point period.

The electricity consumption ($Q_{Elec,GAHP}$) of the GAHP 80K unit were directly measured using a watt node. Each test point was evaluated and converted to power and energy demand for the given test period.

The GAHP 80K hydronic energy output was calculated using Equation 2.

Equation 2: Energy output.

$$Q_{out_f} = \sum \dot{V}_f \cdot C_{p_f} \cdot \rho_f \cdot (T_S - T_R) \cdot \Delta t$$

where

Q_{out_f} = GAHP 80K accumulated energy output, Btu
$\dot{V}_f$ = heating loop flow rate, gallons per minute (gpm)
c_{p_f} = heating loop specific heat as a function of average process temperature and volume base glycol water mix %, Btu/pound-mass (lbm)-°F
ρ_f = heating loop density at the average process temperature and volume base glycol water mix %, lbm/gallon (gal)
T_S = water glycol loop supply temperature, °F
T_R = water glycol loop return temperature, °F
Δt = data logger time-step of 5 seconds, min

With Equation 1 and Equation 2 defined, the gas only COP and the overall system COP (includes electric power consumption) was calculated according to Equation 3 and Equation 4, respectively:

Equation 3: Gas only COP.

$$COP_g = \frac{\dot{Q}_{out_f}}{\dot{Q}_{in}}$$

Equation 4: Overall system COP (including electric power consumption).

$$COP_{GAHP} = \frac{\dot{Q}_{out_f}}{\dot{Q}_{in} + \dot{Q}_{Elec,GAHP}}$$

The COP ratio was calculated by incorporating both the steady state and load-based results according to Equation 5 and Equation 6, respectively.

Equation 5: Gas only COP ratio.

$$COP_g\ Ratio = \frac{COP_{g,load-based}}{COP_{g,SS}}$$

Equation 6: Overall system COP ratio.

$$COP_{GAHP}\ Ratio = \frac{COP_{GAHP,load-based}}{COP_{GAHP,SS}}$$

where

$COP_{g,SS}$ = gas only COP at relative steady state testing parameter.

$COP_{GAHP,SS}$ = overall system COP at relative steady state testing parameter
$COP_{g,load-based}$ = gas only COP at load-based testing parameter
$COP_{GAHP,load-based}$ = overall system COP at load-based testing parameter

The part load percentage (PLR) is represented by Equation 7.

Equation 7: PLR.

$$PLR = \frac{\dot{Q}_{out_f,load-based}}{\dot{Q}_{out_f,SS}} \cdot 100\%$$

where

$\dot{Q}_{out_f,SS}$ = GAHP 80K accumulated energy output at relative steady state testing parameter, Btu/hour (h)
$\dot{Q}_{out_f,load-based}$ = GAHP 80K accumulated energy output at load-based testing parameter, Btu/h

Steady State Evaluation

Steady-state conditions were established for at least 1 hour, with the last half hour at equilibrium. Data was overaged over the last 15 minutes of the test duration. The steady-state raw data is presented in Appendix 2.0 Steady State Results. An example of test trends is shown in Figure 5. In this particular example, the test was started at an OAT 47°F. The GAHP continued to run through an automated sequence through five steady state OAT up to 110°F as described in the steady state test plan matrix.

Figure 5: Timeseries Steady State Data.

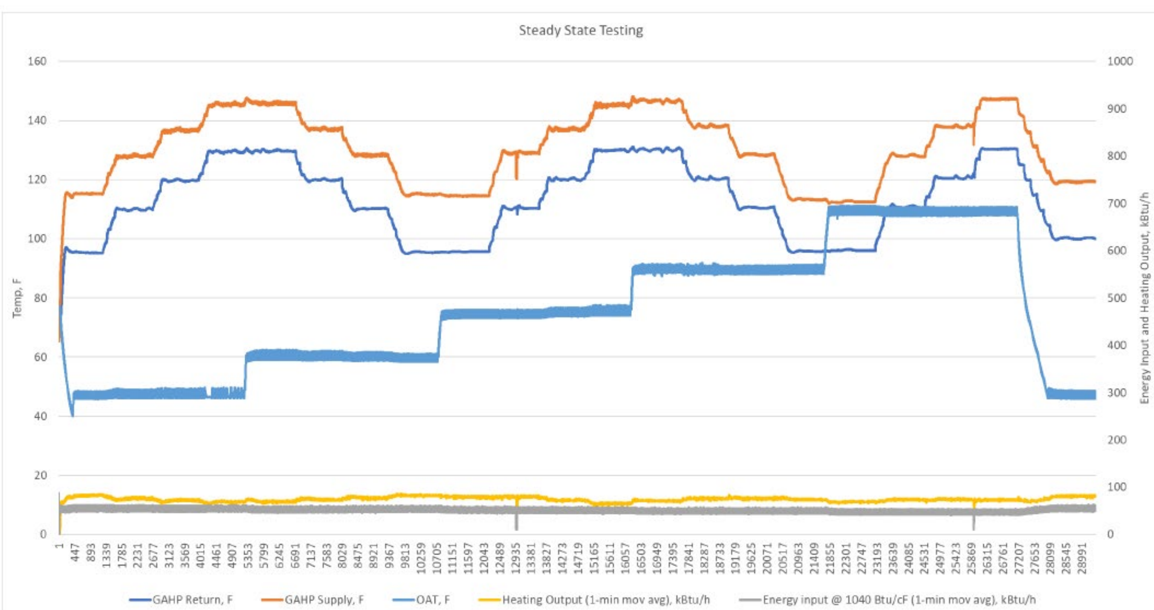

Gas Input

The gas valve was set during commissioning at 30% and 94% firing rates according to manufacturer instructions and not modified. Figure 6 shows the firing rate characterization as a function of ambient operating conditions. Due to density changes between air and natural gas in the premix burner, the firing rate increased slightly at lower OAT. This variation is beneficial as more heating capacity is needed as ambient conditions drop and vice versa. From the commissioning results, it was determined that the full rated firing rate (55 kBtu/h) was achieved at 94% firing rate. The GAHP maximum firing rate is adjustable, set during installation and commissioning, to account for location variable in parameters such as elevation.

Figure 6: Firing Rate vs. OAT.

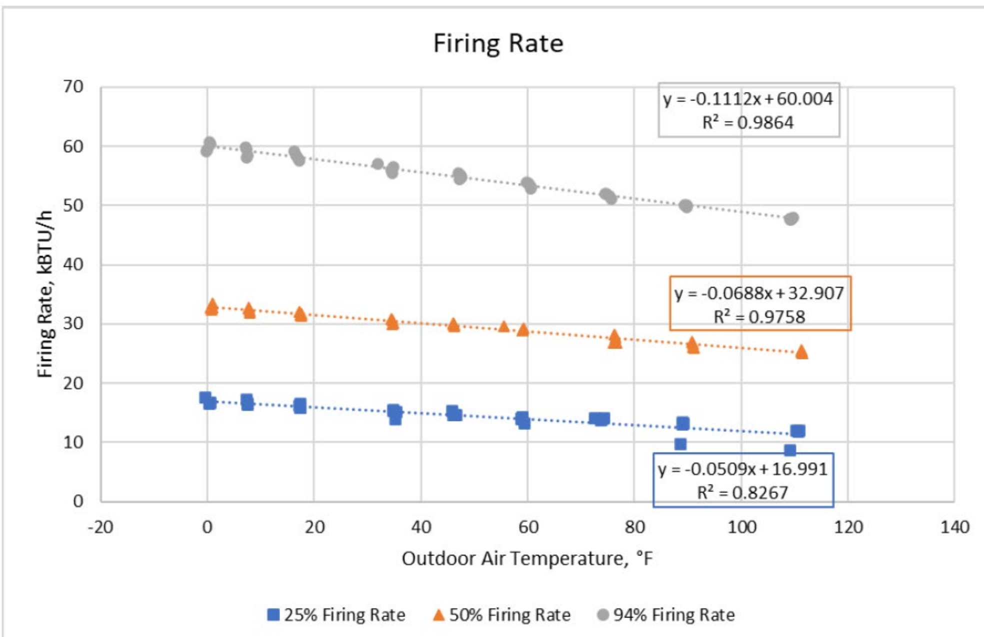

Electricity Input

The GAHP unit requires electrical power for the solution pump, the air coil fan, and the controls. The electricity input was characterized similarly to the gas input. In Figure 7, the electricity input is nearly constant for each firing rate, with slight variation for RTs reflecting flow rates and pressure differences through the solution pump and increases slightly as the ambient conditions drop. The power to the external pump was excluded from this evaluation as it depends on how the unit is installed.

Figure 7: Power Input vs. OAT.

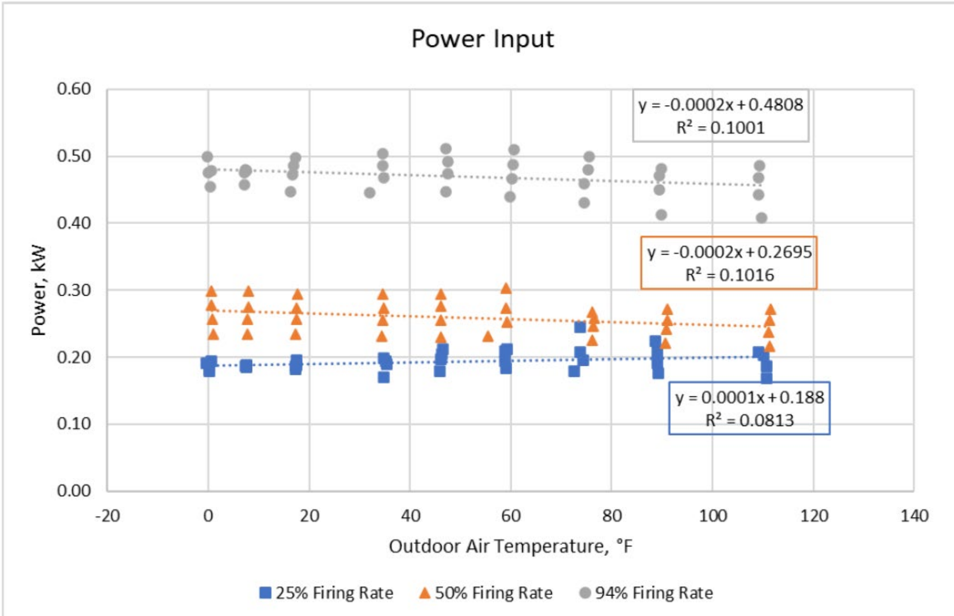

Heat Capacity

Heating output is shown in Figure 8. At full firing rate, the output peaks near the combined variable of the difference of RT and ambient temperature (RT-OAT) of 40-60°F while output for 50% and 25% firing rates was consistent through the range of RT and OAT test conditions. The combined variable is the temperature difference between the heat source (ambient) and the heat sink (hydronic RT), understood as the temperature lift. System design parameters are evidently optimized for a particular thermal lift compared to off-design conditions.

Figure 8: Heating Output vs. RT-OAT.

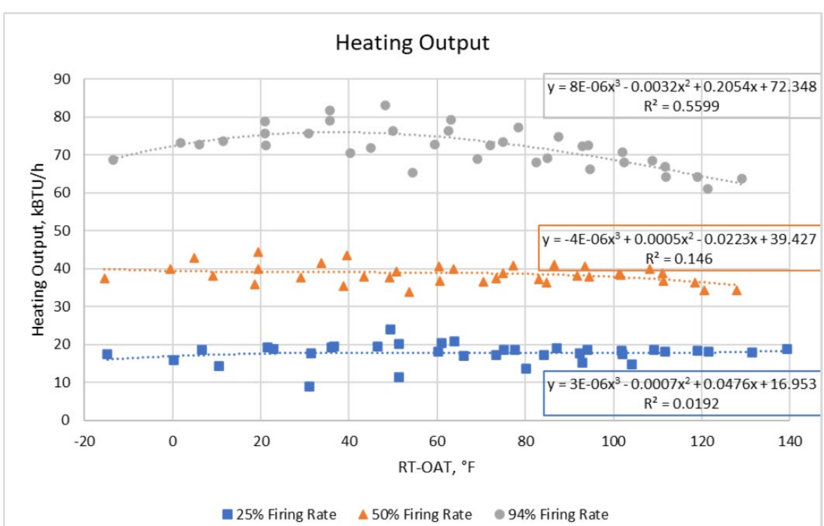

The heating output was then normalized to the rating conditions as described in the Commissioning section of this report. The normalized output uses the ratio between the actual gas input, which varies with the ambient conditions, over the rated gas input of 55 kBtu/h and is used to normalize the energy output at fixed energy inputs. This was plotted against the combined variable RT-OAT. Results are shown in Figure 9, where the full and mid firing rate normalized outputs are closely correlated. The low firing rate output has more variation due to occasional cycling during testing, particularly at the maximum RT of 140°F, shown in Figure 10, due to exceeding the ST limitation which approached 145°F.

Figure 9: Normalized Thermal Output vs. RT-OAT.

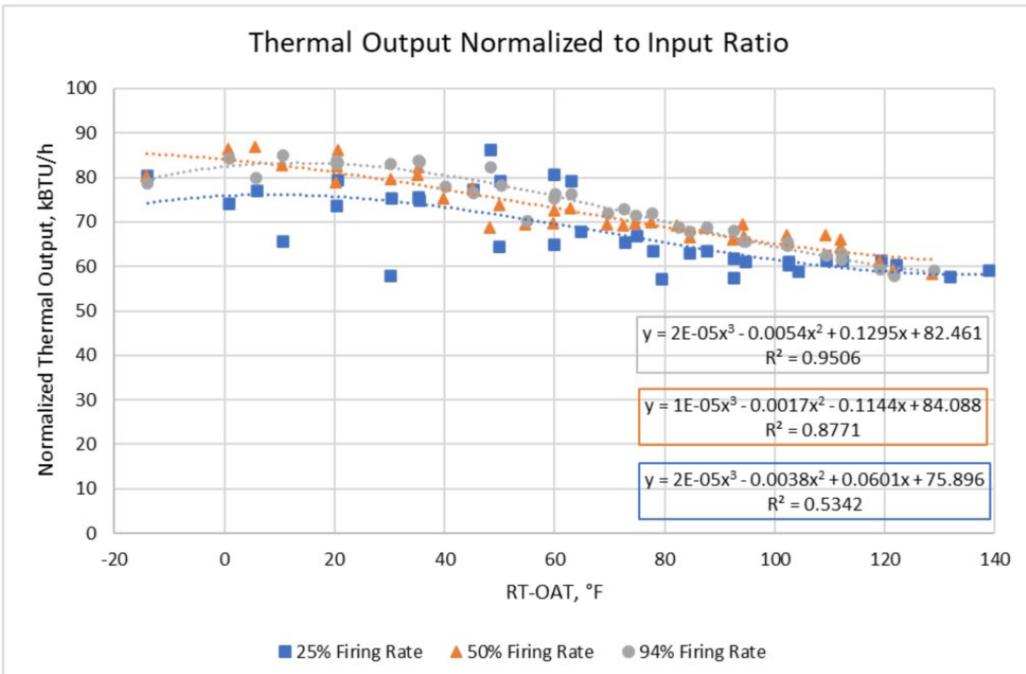

Figure 10: Steady State Trends at 140°F RT.

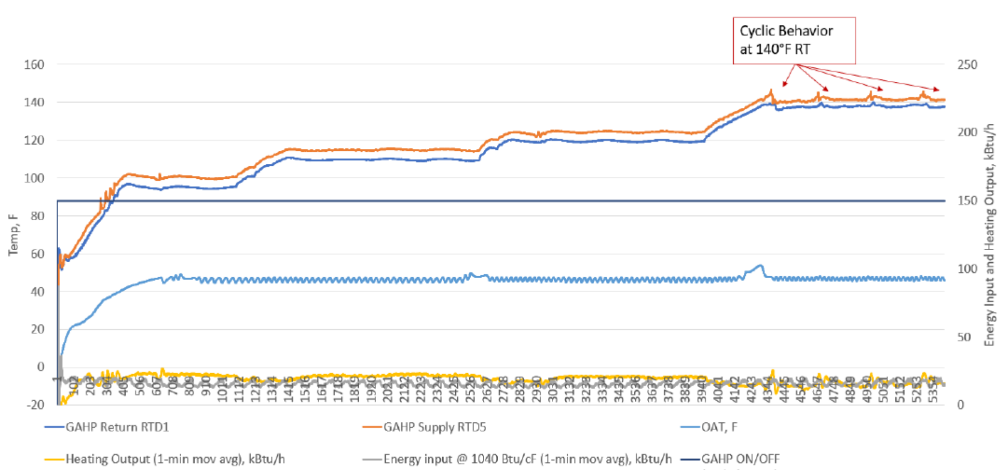

Coefficient of Performance

The test results were further analyzed, and COPs were calculated as described in the Calculations section of this report. The COP (gas-only) and COP (gas + electric) values for the test points are included in Appendix 2.0 Steady State Results. Similar to the normalized thermal output, the high and mid firing rates are closely correlated, with more variation in the low firing rate as shown in Figure 11. The decreasing COP with increasing RT-OAT is consistent with typical heat pump performance where more work is required for increasing temperature lift. Through the range of test points, the COP remained above 1.0, indicating more thermal output than energy input, demonstrating the efficiency benefits of transferring energy from ambient air to the working fluid (glycol) over traditional water heaters or boilers which directly use the input energy to heat the working fluid. At the minimum firing rate, the average reduction in COP is about 5% of the full firing rate, but less than 10% reduction except for a couple outliers which all occurred at the extremes of the operating range, 95°F RT or 140°F RT.

Figure 11: COP (gas-only) vs. RT-OAT.

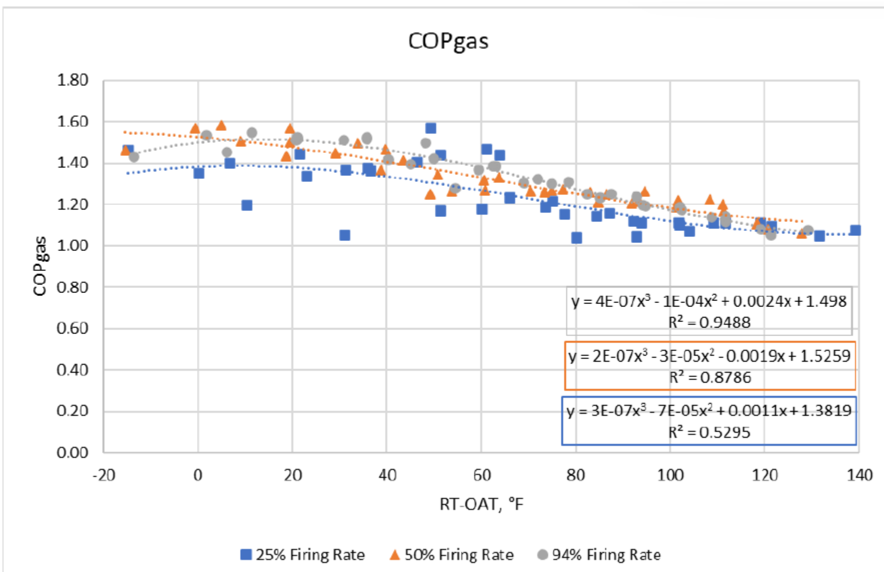

The calculated COPs were consistent with expectations given that at high temperature lift conditions, the heat addition from the evaporator in the GAHP heat pumps is minimal, while the combustion heating is in a condensing mode with an approximate efficiency of 96%. It should be noted that the performance of the GAHP at temperatures below 0°F should be nearly the same as 0°F and not drop further under colder conditions. This can be seen in Figure 12 in that at high RT-OATs (indicated of low OAT), COP becomes nearly constant. This is similar to results from other gas absorption heat pump testing because the heat pump effect becomes very small at low temperatures. This COP pattern contrasts with electric heat pumps, which continually lose capacity and efficiency at lower ambient temperatures. At the lowest RT-OAT, the unit COP reaches its highest value as the GAHP operates at a low lift from the RT to ambient temperatures.

Figure 12: COP (gas + electric) vs. RT-OAT.

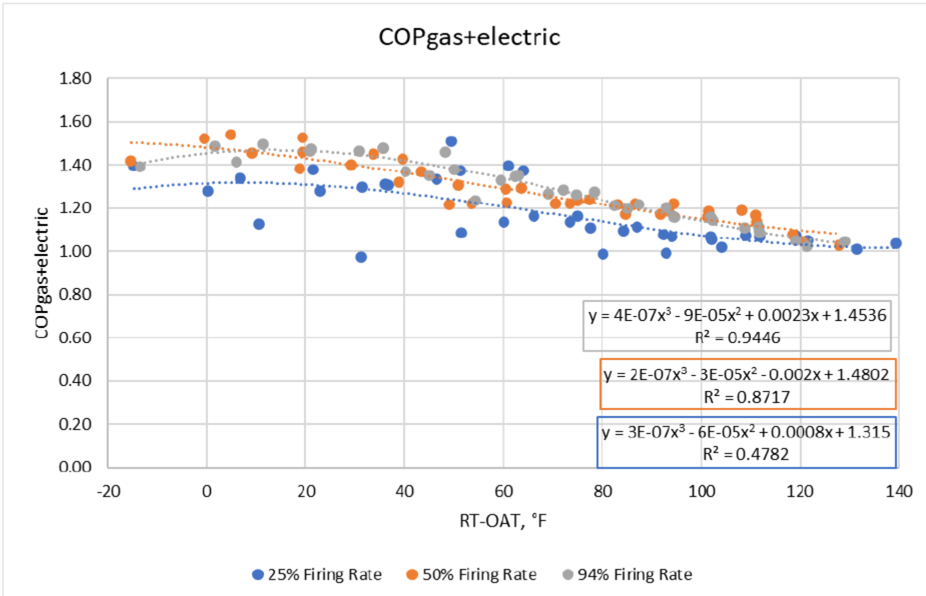

Defrost Characterization

Like all heat pumps, defrost conditions can occur in gas absorption heat pumps near freezing temperatures, particularly when relative humidity levels are high. The GAHP unit's defrost characterization was performed at OATs of 40°F, 30°F, and 20°F at a RT of 110°F. While the environmental chamber experienced unit cooler defrost cycles at this condition, there were no clear defrost cycles of the GAHP since the humidity levels in the environmental chamber were insufficient for this type of test. To address this, a general Filters 5500 model steam humidifier was operated to increase the environmental chamber humidity at frosting temperatures. The steam humidifier injected team into the environmental chamber, with a rated capability of 1.6 to 4.5 kg/h of steam. It was operated to maintain 80% to 100% relative humidity (RH) in the chamber during testing. With the steam humidifier in operation and ducted to direct humid air towards the evaporator coil, various defrost cycles were measured and observed. A total of 4 defrost cycles were tested and measured at an average of 35°F OAT. Figure 13 shows the defrost pattern observed during a defrost cycle at average RH of 80%.

Figure 13: Defrost Characterization Timeseries.

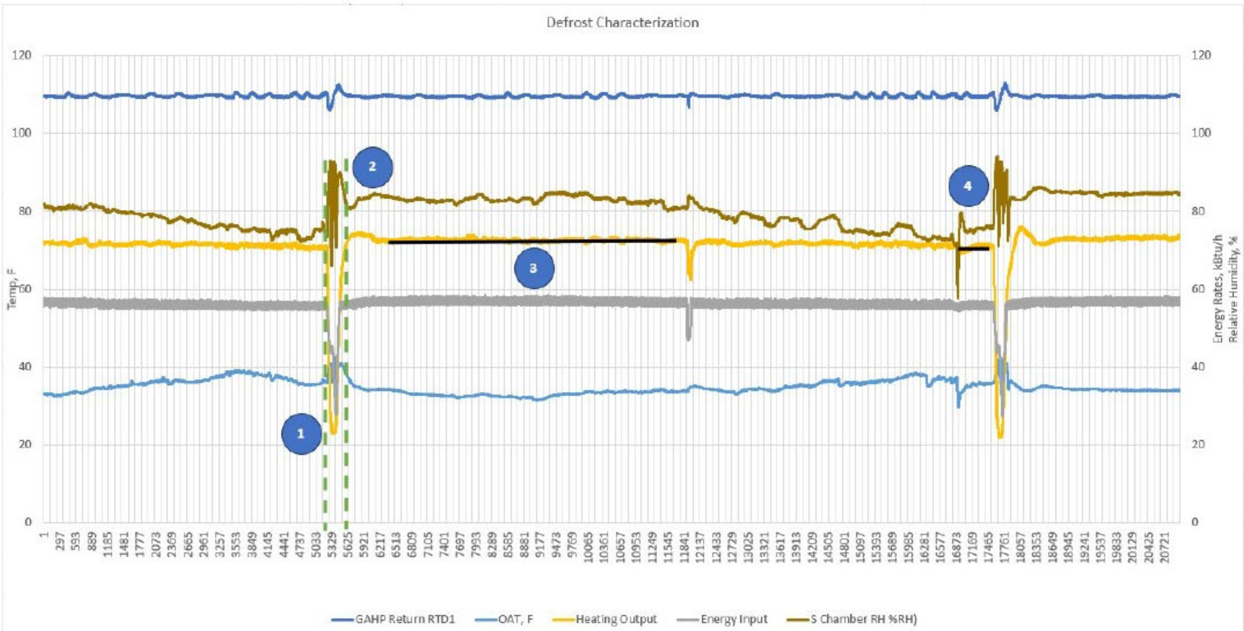

The defrost cycle was characterized by several parameters with rapid change and are described below and summarized in Table 12.

Time Between Defrost Cycles

The time between defrost cycles is defined by points 1 to 4 in Figure 13. The testing performed varied between 15.2 and 17.1 hours, with a mean time of 16.1 hours. Based on the limited testing performed, the time between defrosts can vary significantly and affect performance.

Defrost Cycles Duration

Figure 13 defines the duration of a defrost cycle from points 1 to 2. Across the four defrost cycles evaluated, the testing performed showed a relatively constant duration of 21.8 to 33.3 minutes from the time defrost was initiated until the heating capacity returned to the pre-defrost level, with an average duration of 26.5 minutes.

Average Heating Output Derate During Defrost

Figure 13 defines the average heating output during defrosting from points 1 to 2. This value also demonstrates the impact of a defrost cycle. A noteworthy finding is that the heating output did not drop to zero during a defrost cycle. In fact, from start to finish of the 26-minute defrost cycle, the heating capacity was 60% of its pre-defrost capacity (from 72.8 kBtu/h to 43.3 kBtu/h).

Average Heating Output Prior to a Defrost Cycle

The average heating output derate prior to a defrost cycle is defined as the ratio between the heating output at point 4 and the energy output at point 3 in Figure 13.

Average Defrost Derate on a Heating Cycle

The average defrost derate on a heating cycle is defined as a difference between performance from point 1 to 4 over steady-state performance. This derate varied between 0.6 to 1.4%, with an average of 1.0%

These defrost results suggest additional evaluation is needed to properly characterize defrost derate across multiple operating conditions, e.g., 0 to 40°F OAT and 40 to 100% RH levels. Therefore, the overall impact with an average of 1.0% derate is minimal relative to electric-driven heat pumps of up to 15% [5]. Examples of capacity reduction in cold-climate air source heat pumps show 9 to 15% drops because of defrost [6].

Table 12: Defrost Characterization at 35°F OAT.

Defrost Tests	Target Operating Conditions	OAT, °F | RH, %	Cycles	Time Between Defrost Cycles, hr	Avg. Time Between Defrost Cycles, hr	Avg. Defrost Cycle Duration, min	Avg. Heating Output Derate During Defrost Cycle, %	Avg. Heating Output Prio to a Defrost Cycle, %	Avg. Defrost Derate on a Heating Cycle, %
1	110°F RT	34.5 | 80.2	4	15.2	16.1	26.5	40%	94%	1.0%
		34.5 | 80.1		17.1					
		34.4 | 81.4		15.9					
		34.3 | 80.3		16.2					

Load Based Evaluation

Load based test results were evaluated relative to the ANESI GAHP 80K steady-state performance testing discussed in the Steady State Evaluation section. The load based raw data is presented in Appendix 3.0 Part Load Results.

Unit Replacement and Impact on Results

After completing both steady state and load-based testing, the unit was idle for several months. When testing was re-initiated for the next project, a drop in performance was noted. After reviewing the data and discussion with the OEM, it was decided to replace the unit.

When the replacement unit was recommissioned and baseline testing performed, load-based performance improved significantly, as can be seen in Figure 14. This can be attributed to two changes: (1) an improved expansion valve control algorithm was incorporated and showed reduced hunting (i.e., oscillations) during transients, (2) as noted previously, the original unit experienced refrigerant contamination and periodic reduced performance. The expansion valve was cleared by cycling it while fully open, but contamination may have played a role in reduced performance at part load.

Figure 14: Original vs. Replacement Unit Part-Load Performance.

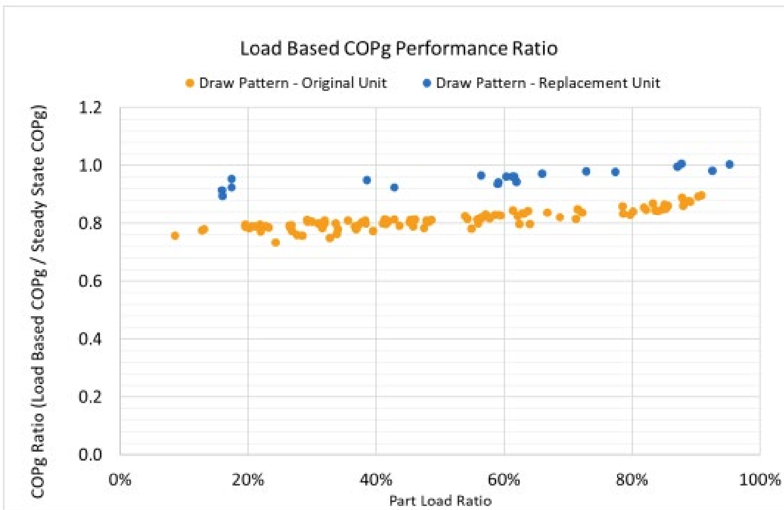

The full range of test conditions was repeated with the replacement unit, with fewer repeat tests. The results presented are based on the replacement unit's performance.

Steady State Reduced Firing Performance

Testing at steady state with a reduction in the firing rates resulted in part-load performance as shown in Figure 15. At 50% firing, the unit COP was nearly identical to 100% firing, and at 25% firing, the unit COP drops only slightly before reaching the minimum turndown ratio below which unit cycling occurs. The design of the ANESI GAHP 80K unit, incorporating an electronic expansion valve (EEV), provided high performance while modulating to lower capacities. This implies added complexity but improved off-design performance compared to fixed firing rate units.

Figure 15: Reduced Firing Rate Performance.

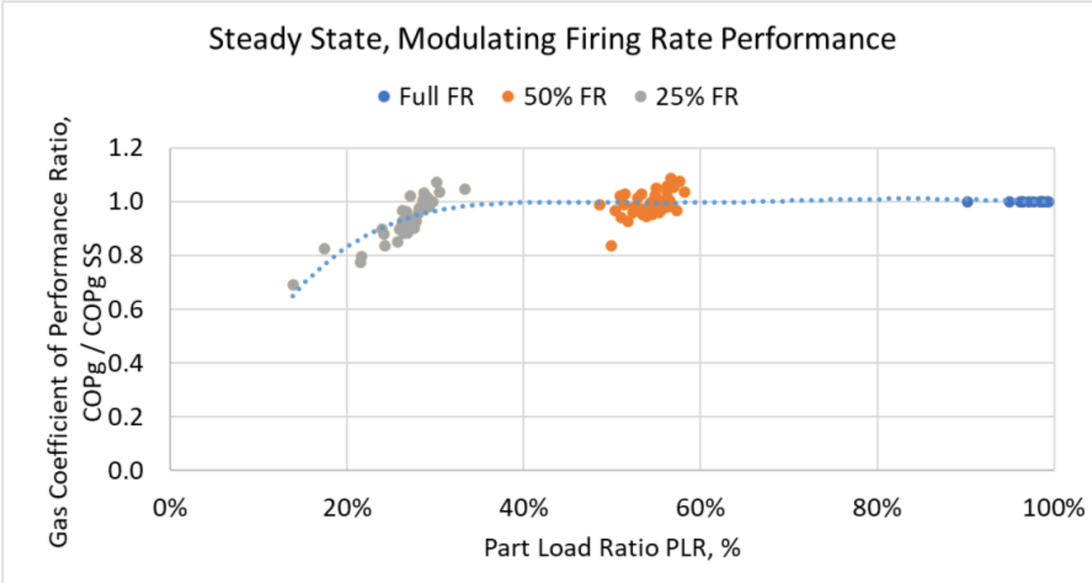

Note that the load-based test setup was modified from the steady state configuration to integrate a 119-gal storage tank with an internal heat exchanger based on Stone Mountain Technologies Institute's (SMTI)recommended operational approach. This configuration update is shown in Figure 16.

Figure 16: Load-Based Testing Configuration.

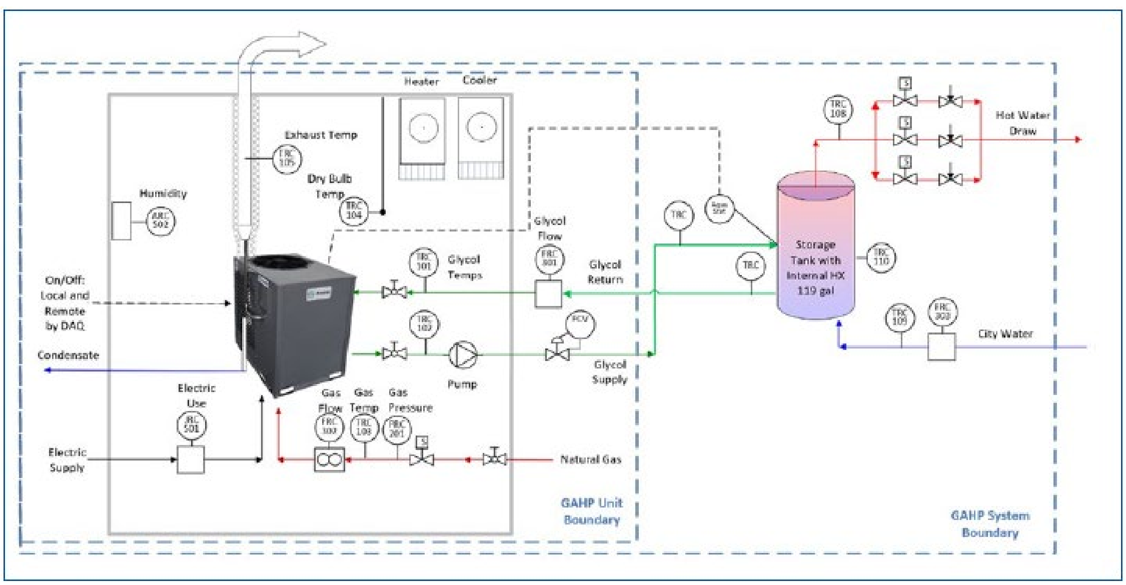

Standby Losses

With the unit in the revised configuration according to Figure 16, testing was controlled by an automated program with varying hourly water draws to align with the test matrix. To determine the standby losses of the tank, the program initiated a water draw to induced the GAHP to cycle on and heat the tank until the aquastat was satisfied, which cycled the unit off, and resulted in the starting point of the standby loss cycle. The system was monitored through the next heat call and completion of the GAHP heating cycle. With no water draw, the system averaged 40-minute run times to heat the tank at 120°F aquastat setpoint, and 68 minutes at 140°F aquastat setpoint. Standby testing was performed with aquastat temperatures of 120°F and 140°F and three OATs. Note that the OAT affected the GAHP unit, while the indirect tank was at room temperature. Figure 17 depicts a representative plot of the standby loss results.

Figure 17: Timeseries for Standby Loss Testing.

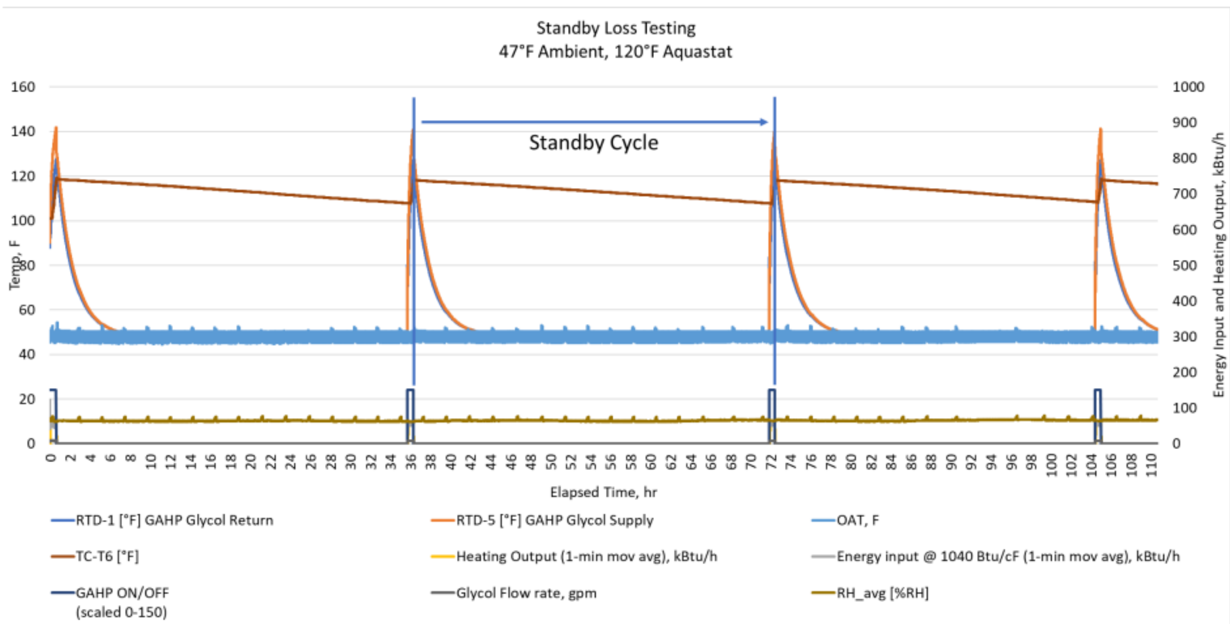

Based on the results, the losses from the tank were calculated to be 8.3 Btu/h.°F with the tank aquastat set to 120°F and 12.0 Btu/h.°F with the tank aquastat set to 140°F, which is representative of typical tank heat losses. This results in lower losses than promoted by the OEM tank, whose data sheet states heat losses to be less than 0.5°F per hour [9]. Published information for the aquastat indicated a deadband of 8°F, however, during the standby cycle, the unit cycled when the internal temperature dropped by approximately 10°F. During further testing presented below, it can be seen that the on/off cycling control points vary by more than 10°F, indicating that other factors such as temperature lag in the thermowell and aquastat, as well as internal stratification likely play a role in this deadband.

Low Draw Testing

Following standby loss testing, low draw testing evaluated system performance when the demand was less than the rated load at the minimum modulation ratio of the ANESI GAHP

80K unit. The tested draw rates (12 and 24 gal/h) were chosen to represent approximately 10% and 20% of the unit rated capacity, with the unit operating on a call for heat and cycling off when the aquastat set point is reached. When designing the test, it was believed that the unit would fire at the minimum rate to minimize on/off cycling, but the system controls were designed such that the unit fires at 100% until either the call for heating was met or the glycol ST reaches 140°F and the firing rate was reduced.

The test began with a water draw of approximately 0.5 gpm and was stopped after reaching the 12- or 24-gallon draw (24 and 48 minutes, respectively). A heating call was induced when the aquastat detected that the water temperature was below the setpoint. Test data was recorded during the entire cycle. For each water draw and test conditions, at least 3 cycles were observed with the first one ignored.

Figure 18 shows a representative results plot. Tank draws can be seen at the bottom of the chart, starting with 12 gal/h and concluding with 24 gal/h. Across the test matrix, the minimum cycle time for the 12 gal/h tests and the 24 gal/h tests are approximately 28 min and 32 min, respectively. Energy input (grey line) shows the relatively short duration firing, with the resultant energy output (yellow line) nearly overlapping, thus indicating the COP would be approximately 1.25. TC-T6 is the measurement of the internal tank temperature at the midpoint which is at the approximate height of the aquastat. For the test shown, the aquastat setting was 120°F with the measured results being approximately 119.5°F. Compared to the steady temperature decline in the standby test, tank stratification is evident in the low draw test.

Figure 18: Timeseries for Low Draw Testing.

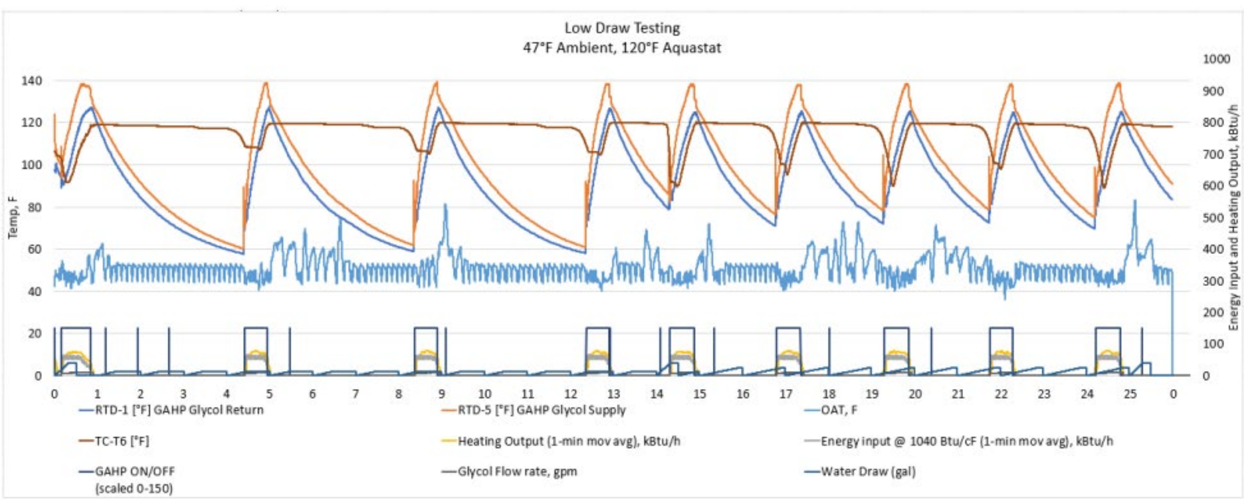

Figure 19 shows internal tank temperature stratification during a single cycle, with TC-T6 boldened in green. A temperature sensor tree with 12 thermocouples was installed in the tank, with TC-T1 being the lowest and evenly spaced to TC-T12 being the uppermost. A representative time plot showing internal temperatures is shown, with the city water temperature approximately 70°F during low-draw conditions of 12 gal/h. The tank filling with cold water can be seen with the lower sensors reaching city water temperature. After about 40 gallons of water draw or 1/3 of the tank capacity, there's a rapid decline in temperature at TC-T6, approximately the position of the tank aquastat. At 4 hours, the heat pump cycles on and the tank temperatures begin cycling.

Figure 19: Tank Stratification.

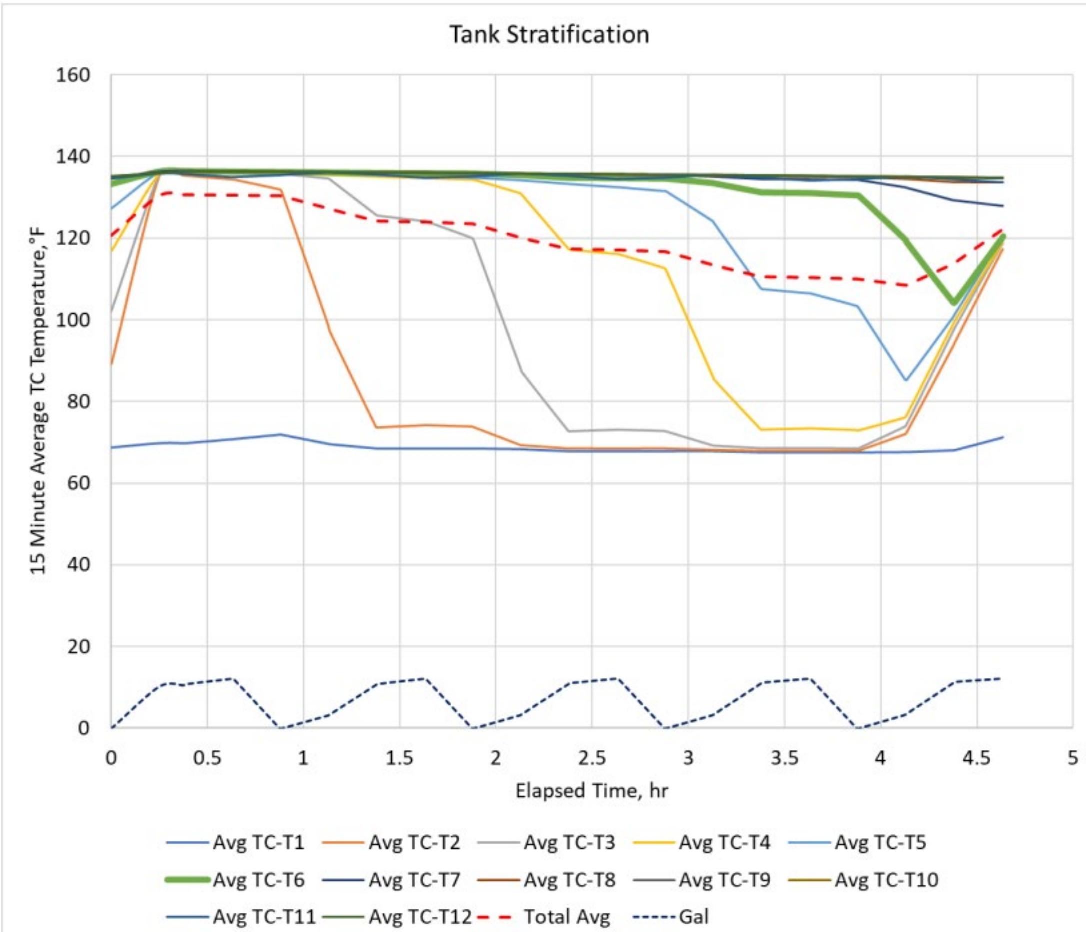

The results of steady state reduced firing rate, standby testing and low draw testing are shown in Figure 20. Steady state results at 50% and 25% firing a minimal drop in COP. For further reduced load (low-draw and standby), COP continues to drop, with the minimum a minimum value of approximately 0.75 for standby conditions.

Figure 20: Steady State Low Firing Rate Comparison to Load Based Performance.

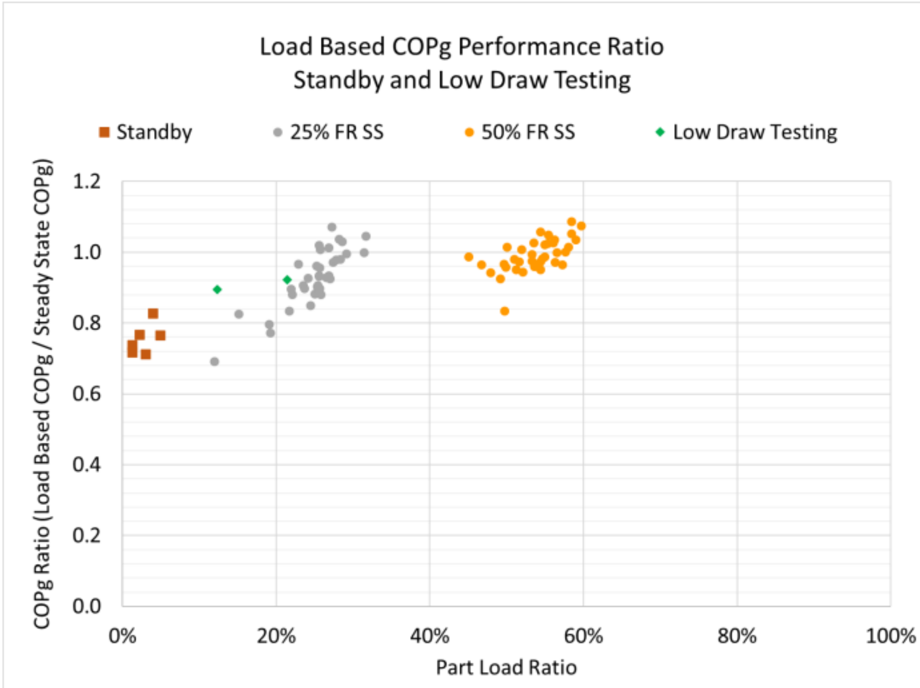

Draw Pattern Testing

The final test sequence was run using an automated hourly draw pattern over 24 hours, repeated sequentially for three days for each of the test conditions. This draw pattern was used with draws of 1,000, 3,000, and 5,000 gallons per day (gpd) according to Figure 1. The first day's results were ignored, and the 2 remaining days were averaged. Results were analyzed for the entire day and also on a per cycle basis, using data from each GAHP cycle, from the end-to-end of a cycle. Figure 21 presents results from a representative day shown for 3,000 gpd at an aquastat setting of 120°F.

Figure 21 shows water draws at the green curve with very low draws for the first 6 hours, and the highest draws in hours 7-9. The GAHP on/off condition is shown. Note that during the first 6 hours, the unit operates intermittently to maintain tank temperature but operates continually during hours 6-11 and 19-23. During hours 11-18, the unit operates more than 50% of the time. Resulting glycol and water temperatures are shown in the 80°F to 140°F range with the GAHP ST, GAHP RT as the higher curves and water temperature at the mid-point of the tank (TC-T6) tracking the glycol temperatures. Noteworthy is the cycling operation with the glycol ST rising during operation, peaking at approximately 140°F and cycling to maintain glycol temperatures within the unit's parameters. Unit performance (presented as gas COP (COP_g) scaled by 100x, calculated as the measured energy output from the GAHP based on glycol flow rate and temperature differential, and measured gas consumption) is shown for 1-minute averages and as relative to steady-state performance.

Figure 21: Timeseries for Draw Pattern Testing.

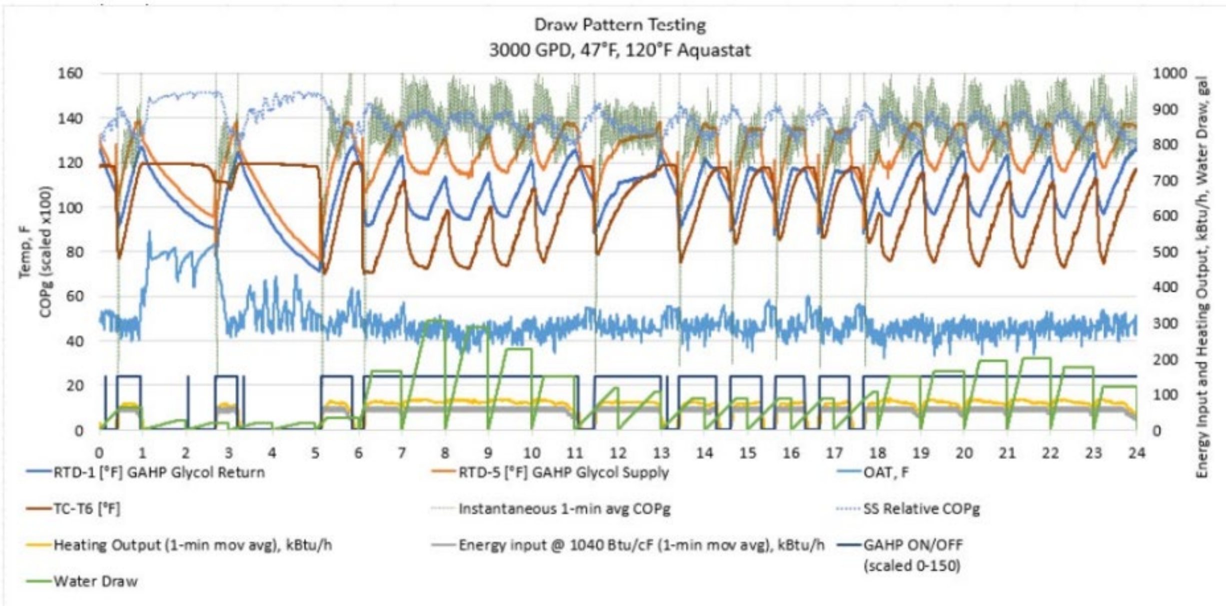

Figure 22 zooms in on the prior chart from hour 6 to hour 12 to highlight the dynamics of the draw pattern. The instantaneous COP_g is shown and scaled to a trailing 1-minute average. As the water draw (shown in solid green) concludes for each scheduled hour, the tank temperature recovers, pulling up the glycol RT (shown in solid blue). Two observations of the data follow:

1) During the high draw periods (hours 7-10), the unit was operating at 100% but was not able to meet demand. The ST drop can be seen during these periods to be as low as 80°F. A detailed temperature profile of the water tank is shown in Figure 23.
2) During the latter period of an active water draw, the glycol RT is relatively stable (shown in solid blue). The instantaneous trailing 1-minute average COP_g approaches the equivalent steady state COP_g under the same glycol RT and OAT. During this portion of the cycle, the unit operates at the highest COP and drops somewhat as the RT climbs.
3) The vertical red line indicates completion of the draw where RTs begin rising as the tank is reheated. During this phase, both the RT and ST are rising, with the ST approaching the rating maximum temperature.

Figure 22: Draw Pattern Testing Instantaneous COP$_g$.

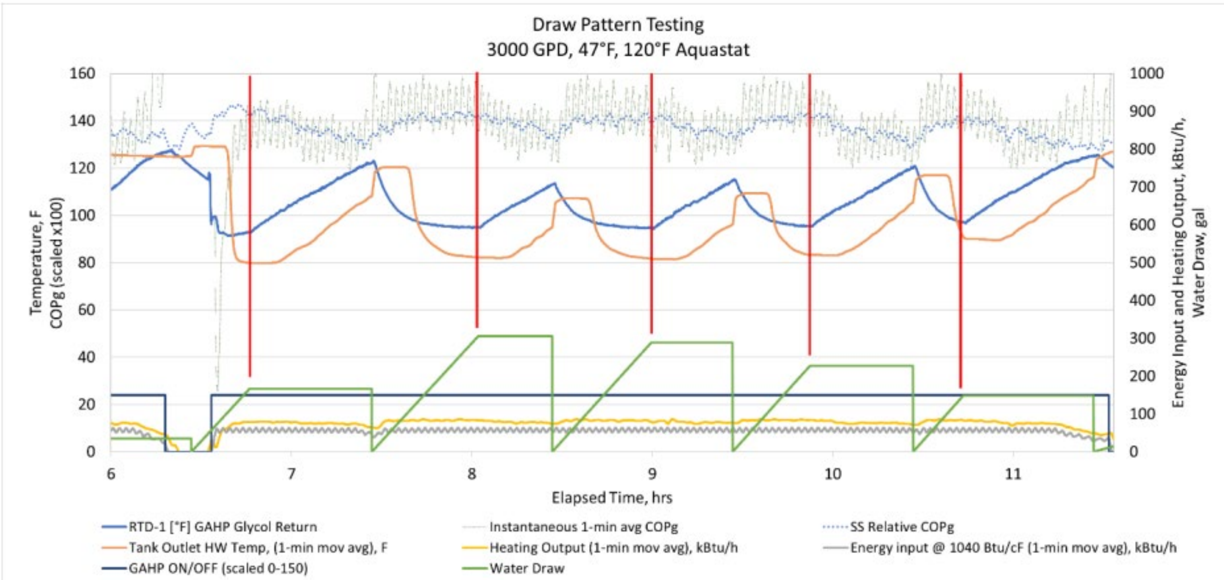

Figure 23: Tank Temperature Profile During 3,000 GPD Draw.

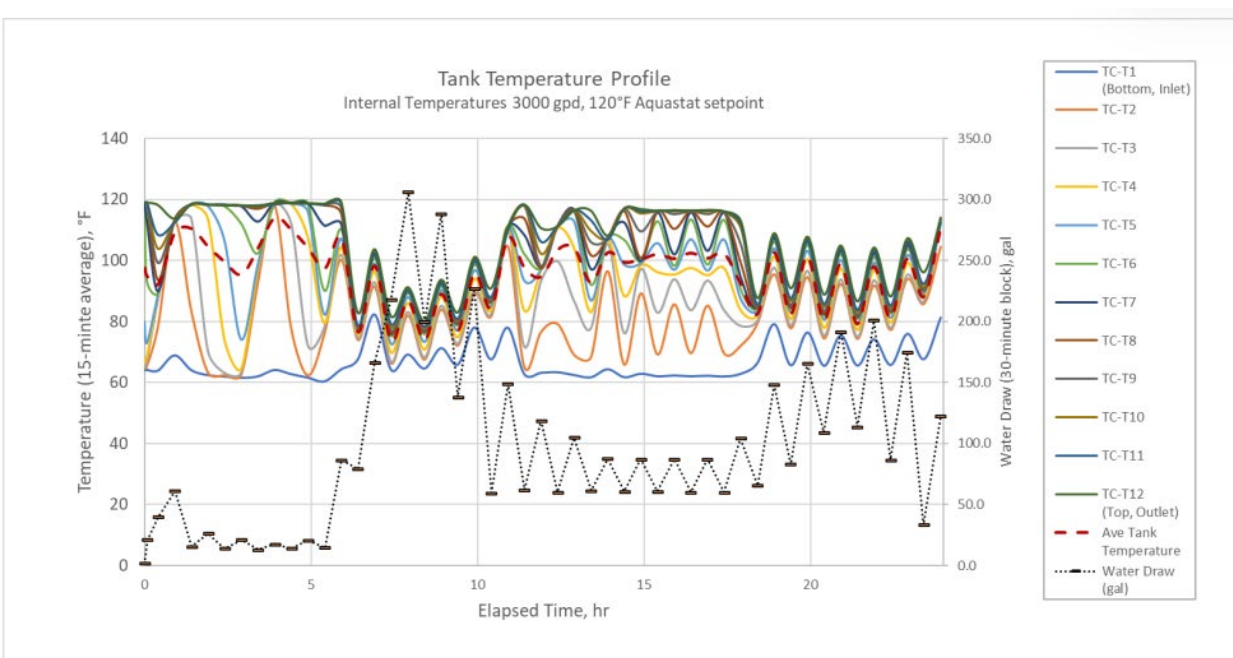

Coefficient of Performance

Figure 24 presents the performance ratio for standby, low flow, and draw pattern test results relative to the steady state performance. Results of the COP$_g$ for the load-based tests divided by the COP$_g$ as characterized during the steady state testing shows a linear trend with part load ratio (PLR) ranging from 0.2 to 1.0. PLR is defined as the average load delivered by the GAHP in kBtu/h over a heating cycle divided by the steady state capacity of the GAHP at the average OAT and RT during the cycle. The figure includes results of each heating cycle for the standby, low flow, and draw pattern tests conducted. Also, of note is that the COP_g values presented are of the GAHP unit alone, and do not include other system losses or tank losses.

Figure 24: Load Based COP_g Performance Ratio.

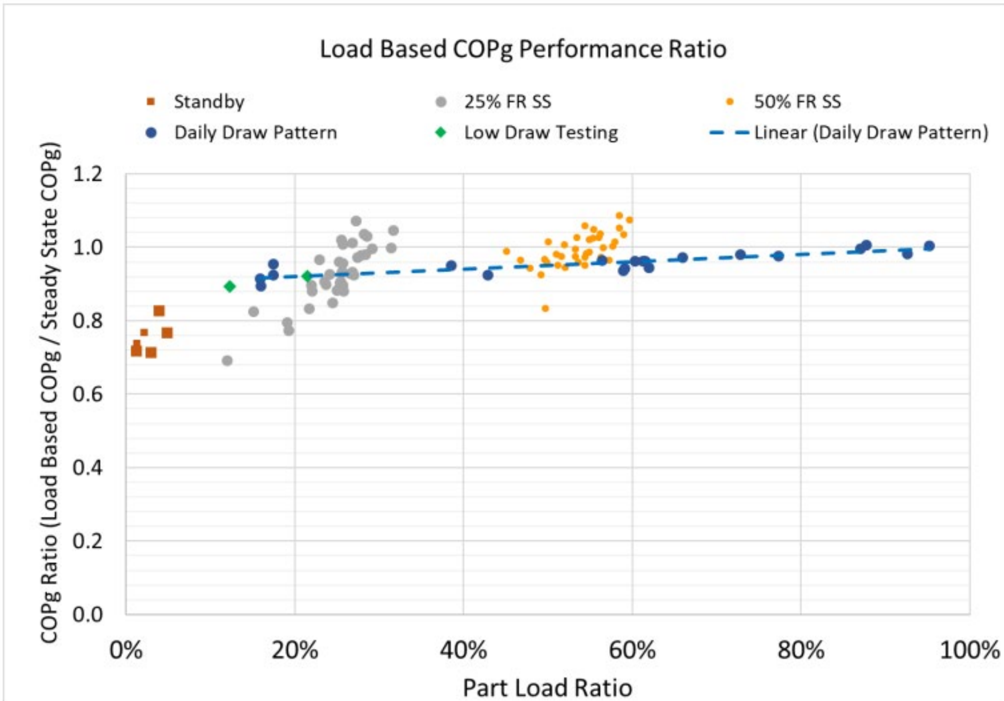

Noteworthy is that the performance of the unit approaches unity over a broad range of PLRs. The unit COP is within 10% of the steady state performance over the range of 20-100%. This is a key benefit of the ANESI GAHP 80K technology which is able to operate at very load PLRs.

As discussed previously, the imposed load profile applied to the system results in the GAHP RT variations. During steady state testing, the RT was controlled to a constant value for the duration of each test point. The load-based test setup more closely resembles an actual installation with an indirect storage tank. Water draws to induce a heating call to the GAHP were initiated each hour of the test until a target water draw volume was reached. Between water draws, the storage tank recovered in temperature, but the next draw pulled the temperature down in a sawtooth pattern. Constantly fluctuating RTs to the GAHP reduced performance slightly due to varying conditions, independent of the load or run time. Table 13 presents the measured daily COP_g values during the full day draw pattern testing.

Table 13: Daily COP_g.

Daily Draw, gph	Aquastat Temperature, °F	COP (Gas-Only)
17	120	1.28
47	120	1.35
90	120	1.38
17	140	1.28
47	140	1.34
90	140	1.37

Overall System Performance

The GAHP system installation, presented in detail previously, can be seen simplified below in Figure 25 where the GAHP unit is piped to the indirect storage tank. The control of the unit is based on OEM recommendations, to initiate heating cycles based on the storage tank aquastat, located in a thermal well approximately mid-tank height. Results presented in the previous sections show the GAHP unit performance over the range of conditions described with heating output defined at the GAHP unit boundary.

Figure 25: Simplified GAHP System Diagram.

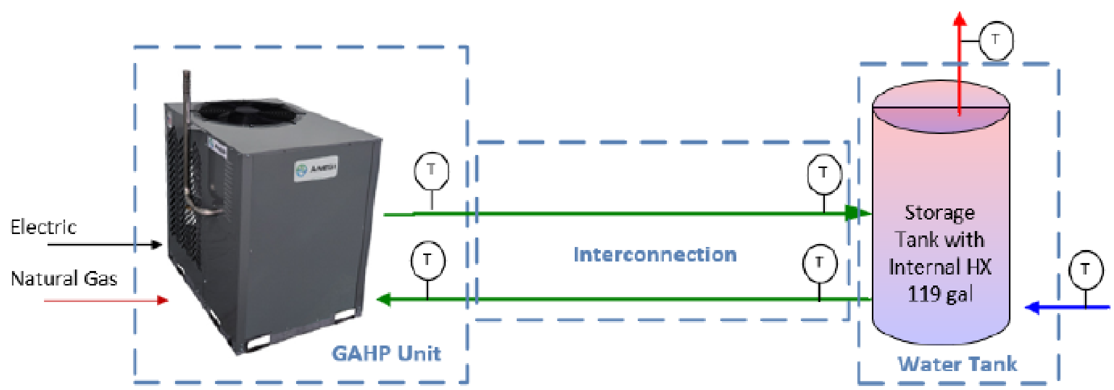

System performance in a field installation also includes heat losses through the interconnection piping and the storage tank. Given that each installation will have different interconnection piping, the laboratory system was used as-is with no efforts made to be representative. The laboratory system was used primarily for heat rejection and thus has much higher heat loss than a typical field installation; the runs are much longer (approximately 75 feet for each of the supply and return piping runs) and are not heavily insulated. Instrumentation is installed to measure temperature and flow rates and thus quantify the heat loss in the interconnecting piping. Heat loss in the storage tank was measured earlier in the standby loss testing.

With this context, the overall system performance for each draw pattern can be shown in Figure 26, showing performance impact over the tested range of conditions – 1,000-5,000 gpd and aquastat settings of 120°F and 140°F. The figure visualized the COP gains and efficiency losses with the thermal output between 1.3 and 1.4 of the thermal input. Thermal losses in both the interconnecting piping and the tank reduce overall efficiency. It can be seen that losses as a percentage are quite low at high draws, but larger at low draws.

Figure 26: Overall System Performance.

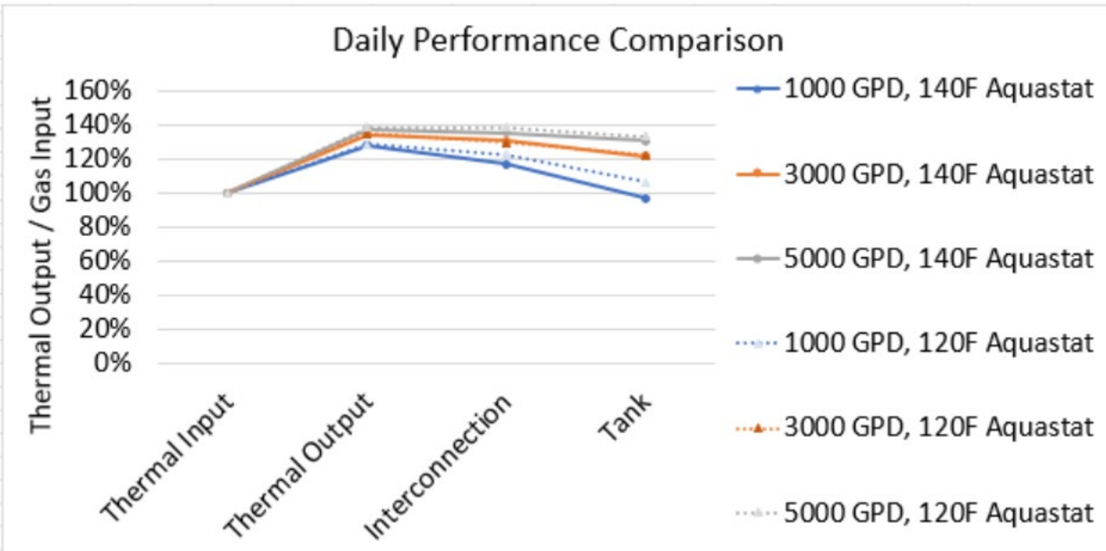

Results presented are applicable with the test setup described in this report. Use of a different tank with more or less heat exchanger surface area will result in different RT profiles and performance. Less coil surface area or an undersized heat exchanger will result in the system operating with higher than necessary RTs, reducing performance. Large surface areas or operating for a longer duration with cooler tank fluid temperatures in the lower portion of the tank (at the heat exchanger return) could improve performance. Tank aquastat position and deadband temperature differential influences the draw volume and its duration. Additionally, the draw patterns, whether intermittent as in this study or longer draws (approaching steady state), also impact the GAHP performance.

Performance representative of a single draw pattern is shown Figure 27. The waterfall chart shows thermal input, thermal output of the GAHP unit, interconnection and tank losses. It can be seen that interconnection losses at 5%, likely typical of many commercial installations, but may not be representative of a specific installation. System losses could be assumed to be based on the unit performance minus tank losses, with a resulting system efficiency of 127% (COP = 1.35 – 8% tank losses).

Figure 27: System Performance 3,000 gpd, 120°F Aquastat.

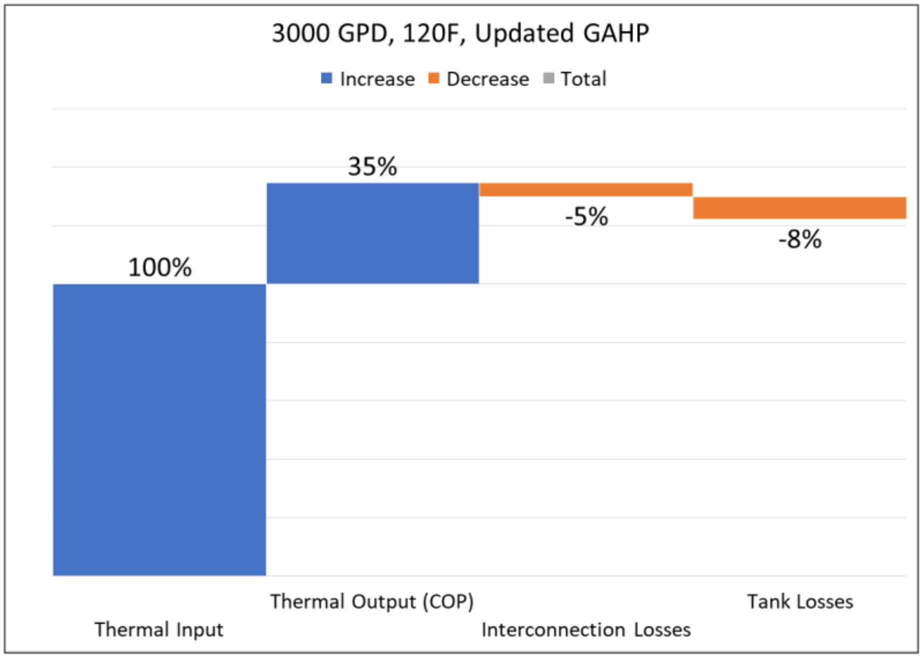

Potential System Improvements

Evaluating the test results, several strategies to improve the performance of the unit have been identified. These improvements largely focus on more steady state operation and operating at reduced temperature lift.

Steady state results in Figure 28 show that the unit COP is highest (1.2 – 1.4) when RT-OAT is 60-110°F.

Figure 28: Steady State COP_g performance.

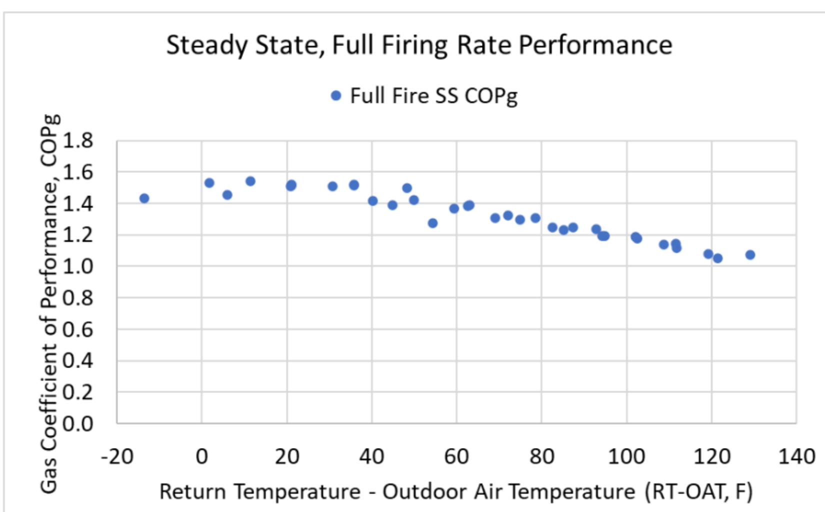

One option to improve performance of the GAHP would be to utilize an external plate heat exchanger between the glycol loop and the tank as shown in Figure 29 instead of a tank with an indirect heat exchanger. Plate heat exchangers achieve very low approach temperatures, reducing GAHP RT, thus improving performance. An additional pump would be required, but this would simplify the storage tank (no indirect heat exchanger needed). An added benefit of this approach is that the heat exchanger can be double wall, eliminating the potential of glycol entering the water loop.

Figure 29: Suggested Configuration with External Heat Exchanger.

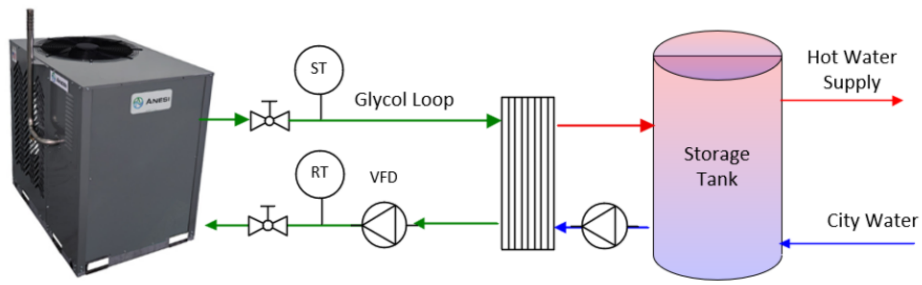

Another performance improvement strategy would be to use several tank water sensors: one at the top, bottom, and one or more in the middle section of the tank. This would allow more comprehensive information of the tank's state of charge and offer the potential of control strategies that optimize run time while meeting hot water demand.

In addition, an arrangement of the GAHP with indirect tank in series with a tankless water heater could be applied. The GAHP would provide the lower temperature lift at high COP, while the tankless water heater could boost the ST during high flow periods or to meet higher STs that may be needed for many commercial applications.

Notable Maintenance Issues

It should be noted that during testing, multiple service calls were needed to address evidence of clogs in the system and resultant reduction in performance. SMTI remote diagnostic capabilities were extremely proficient in identifying and resolving the clogs by noting changes in EEV glide control. Lab assessment by SMTI identified the root cause of contamination being an inadequate factory reclaim process. The reclaim procedure has since been revised to avoid future risk of contaminants entering the system.

When performance results were diverging from prior testing, the typical symptom was high discharge pressure. Service technicians were on site mid-March 2025 to bleed non-condensables at the beginning of April 2025 to replace the EEV and filter, and again at the end of April 2025 where the filter was replaced with a custom filter assembly. This replacement was believed to be sufficient for the remainder of testing. However, after an idle period of several months, when beginning with the next phase of testing, there was evidence of reduced performance and further clogging in a location that was not field replaceable.

A replacement unit was installed at the end of October 2025 for the next phase of testing. Baseline testing indicated significant improvement of the load-based results. Because of this, load-based tests were repeated as described previously. It is believed that both the new control logic as well as eliminating possible clogging have resolved system performance issues.

EnergyPlus Modeling

Results from the steady state and load-based laboratory testing have been used to develop performance characterizations for EnergyPlus modeling. GTI Energy developed these curves using the "Pathways to Decarbonization of Residential Heating" [7]. Calculations used to develop these curves are outlined in the following section and the corresponding constants derived can be found in Appendix 4.0 EnergyPlus Modeling Coefficients. Based on the designed test plan, limitations in the modeling equations include:

- Heat transfer fluid properties are based on a water-propylene glycol mix with a concentration of 37% flowing 8.5 GPM.
- Ambient temperature ranges between 0°F and 110°F.
- Performance is specific to the GAHP only. System performance when integrated with a storage tank requires including tank specific EnergyPlus modules and interconnecting piping and pumping loops; both of these components are outside the scope of this project.

The EnergyPlus module has two independent input variables: ambient dry bulb temperature (T_{amb}) and hydronic return temperature (T_{ret}). Within the range of test results, a function (CAPFT) of these two variables outputs the maximum capacity of the GAHP 80K when multiplied by the rated capacity at standard operating conditions (47 °F ambient and 95 °F RT).

At each time step in an EnergyPlus simulation, the load demand is given and used with the maximum capacity to set a PLR. Several functions are provided to determine the overall gas usage as a function of the two input variables, T_{amb} and T_{ret} (EIRFT), as a function of the PLR (EIRFPLR), and defrost cycle derate (EIRDEFROST) when ambient temperatures are between -8.89°C and 3.33°C (16°F and 38°F). The COP (gas-only) can be determined from the gas usage and heat delivered at any given operating conditions of the input variables and PLR. Similar to gas usage, electric consumption is determined as a function of the two input variables, T_{amb} and T_{ret}, ($AUX_{ELEC,EIRFT}$) and a function of the PLR ($AUX_{ELEC,EIRFPLR}$). The COP (gas+electric) with combined gas and electric consumption equals the rate of heat delivered (kBTU/h) divided by the sum of the energy consumed (gas and electricity converted to kBTU/h).

A key observation between the steady state and part-load testing has to do with the overall test setup. The steady state tests utilized a facility heat rejection skid to control the glycol RT to a set value and duration for each test point. Tests were performed by fixing the firing rate to full fire (basis for steady state performance), and at 50% and 25% firing rates. For the load based testing, the configuration was modified to more closely resemble a field installation. The glycol loop from the GAHP was connected to an indirect storage tank recommended by SMTI (i.e., ANESI) and controlled by the tank aquastat. City water replenished the tank during scheduled water draws, pulling the tank temperature down until reaching the aquastat deadband, located near the midlevel of the tank, creating a demand for heat from the GAHP. As the tank temperature recovered, the glycol loop RT followed, creating a non-steady RT to the GAHP regardless of the GAHP run time. Due to the transient effects, system performance as a function of PLR did not reach unity with the steady state performance. For the EnergyPlus correlations that follow, the GAHP performance at 50% and 25% firing rates were used to characterize the part load performance. Effects of the load based configuration require stratified tank modules and interconnecting pip and pumping modules, and this is beyond the scope of the current project.

EnergyPlus Performance Curve Development

Heating Output Rate

The following outlines the equations used to develop EnergyPlus performance curves based on the lab data and analysis. The GAHP-A heating capacity outlined in Equation 8 is used to calculate the part-load performance in EnergyPlus. The capacity is also used to estimate the gas input and power utilization of the GAHP which are both outlined in Equation 10 and Equation 16, respectively.

Equation 8: Heating Output Rate.

$$GAHP\ Heating\ Capacity = RatedCapacity \cdot CAPFT$$

where

$GAHP\ Heating\ Capacity$ = heating capacity output rate, kilo British thermal unit (kBtu)/h
$RatedCapacity$ = 83.0, kBtu/h
$CAPFT$ = heating capacity correction factor as a function of ambient and return temperature (Equation 9).

The heating capacity correction factor (CAPFT) is calculated using Equation 9.

Equation 9: CAPFT.

$$CAPFT = a1 + b1 \cdot Tret + c1 \cdot Tamb + d1 \cdot Tret^2 + e1 \cdot Tret \cdot Tamb + f1 \cdot Tamb^2 + g1 \cdot Tret^3 + h1 \cdot Tret^2 \cdot Tamb + i1 \cdot Tret \cdot Tamb^2 + j1 \cdot Tamb^3$$

where

$Tamb$ = ambient temperature, °F
$Tret$ = GAHP 80K return temperature, °F
i_1 = coefficients listed in Appendix 4.0 EnergyPlus Modeling Coefficients (Table 23)

Gas Input Utilization

The GAHP 80K gas input utilization is calculated according to Equation 10, including the nominal fuel-based COP. Nominal fuel based COP is an input in the *HeatPump:AirToWater:FuelFired* module in EnergyPlus 23.1.

Equation 10: Gas Input Utilization.

$$GAHP\ Gas\ Use = \frac{\frac{Load}{COP_{nom}} \cdot EIRFT \cdot EIRFPLR \cdot EIRDEFROST}{CRF}$$

where

$GAHP\ Gas\ Use$ = gas input rate, kBtu
$Load$ = EnergyPlus heating load as a function of time, kBtu
COP_{nom} = Rated GAHP capacity / Rated Gas Input, equivalent to 1.498
$EIRFT$ = gas input ratio as a function of ambient and return temperature (Equation 11/Table 24)
$EIRFPLR$ = gas input utilization correction factor as a function of part-load (Equation 12/Table 25)
$EIRDEFROST$ = gas input utilization correction factor as a function of defrost operation (Equation 14)
CRF = gas input utilization correction factor as a function of cycling operation for modulating equipment (Equation 15/Table 26).

The gas input utilization correction factor as a function of temperature (EIRFT) is calculated using Equation 11.

Equation 11: EIRFT.

$$EIRFT = a2 + b2 \cdot Tamb + c2 \cdot Tamb^2 + d2 \cdot Tret + e2 \cdot Tamb \cdot Tret + f2 \cdot Tamb^2 \cdot Tret$$

where

i_2 = coefficients listed in Appendix 4.0 EnergyPlus Modeling Coefficients (Table 24)

The gas input utilization correction factor as a function of part load ratio (EIRFPLR) is calculated as a linear function of PLR using Equation 12 and Equation 13.

Equation 12: EIRFPLR.

$$EIRPLR = a3 \cdot PLR + b3$$

where

PLR = part-load ratio calculated using Equation 13.
i_3 = coefficients listed in Appendix 4.0 EnergyPlus Modeling Coefficients (Table 25)

Equation 13: PLR.

$$PLR = \frac{Load}{GAHP\ Heating\ Capacity}$$

The defrost factor (EIRDEFROST) is calculated using Equation 14. Note that we recommend implementation of this equation as it is referenced in the "Pathways to Decarbonization of Residential Heating" source [7].

Equation 14: Defrost Factor.

$$EIRDEFROST = -0.0011 \cdot Tamb^2 - 0.006 \cdot Tamb + 1.0317\ for - 8.89℃ \leq Tamb \leq 3.333℃$$

The gas input utilization cycling correction factor (CRF) is calculated using Equation 15.

Equation 15: Gas Input Cycling Correction Factor.

$$CRF = a4 \cdot CR + b4$$

where

CR = the cycling modulating derate factor equals the PLR / PLR_{min}, valid in the PLR range from 10% to 25%
PLR_{min} = 25%
i_4 = coefficients listed in Appendix 4.0 EnergyPlus Modeling Coefficients (Table 26)

The effect on COP of the two factors for part load correction, EIRFPLR and CRF, can be seen in Figure 30, with EIRFPLR applied from 25-100% part load and CRF applied from 20-25%.

Figure 30: COP ratio for Part Load Using EIRFPLR and CRF.

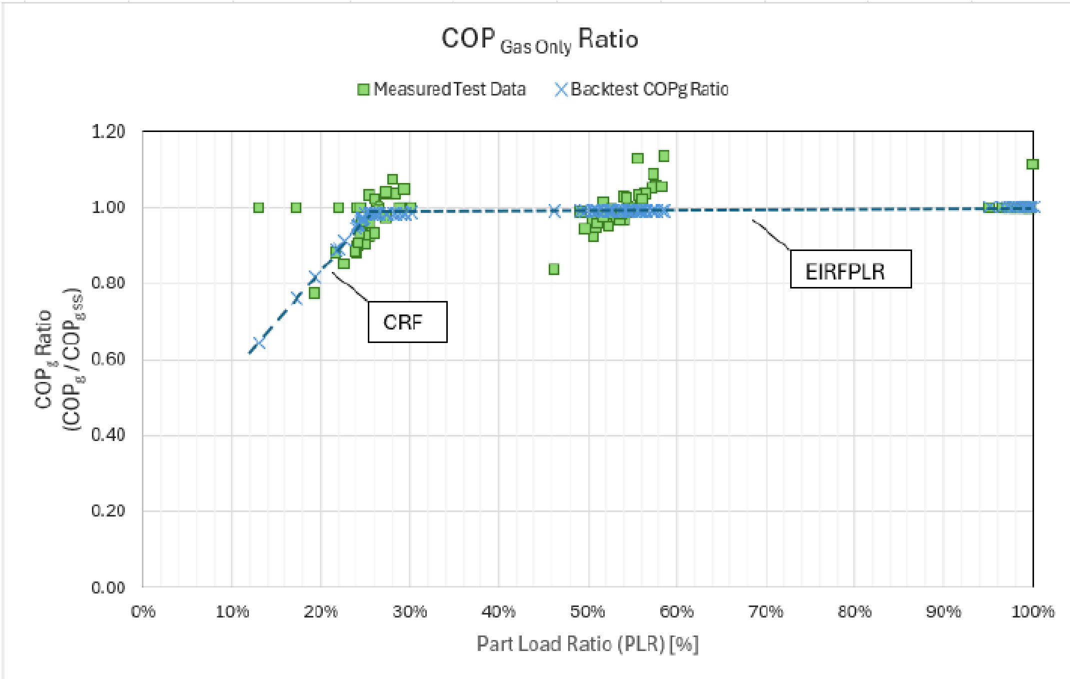

Power Input Utilization

The GAHP 80K power input utilization is calculated using Equation 16.

Equation 16: Power Utilization.

$$Electric\ Power\ Consumption = RatedPower \cdot Aux_{Elec,EIRFT} \cdot Aux_{Elec,EIRFPLR}$$

where

$Electric\ Power\ Consumption$ = power input utilization, kWh
$RatedPower$ = 0.446, kWh
$Aux_{Elec,EIRFT}$ = power input utilization correction as a function of return and ambient temperatures
$Aux_{Elec,EIRFPLR}$ = power input utilization correction factor as a function of part-load

The power input utilization operating conditions correction factor ($Aux_{Elec,EIRFT}$) is calculated using Equation 17.

Equation 17: Power Utilization Operating Conditions Correction Factor.

$$Aux_{Elec,EIRFT} = a5 + b5 \cdot Tamb + c5 \cdot Tamb^2 + d5 \cdot Tamb^3 + e5 \cdot Tret + f5 \cdot Tamb \cdot Tret$$

where

i_5 = coefficients listed in Appendix 4.0 EnergyPlus Modeling Coefficients (Table 27)

The power input utilization cycling correction factor ($Aux_{Elec,EIRFPLR}$) is calculated using Equation 18.

Equation 18: Power Utilization Cycling Correction Factor.

$$Aux_{Elec,EIRFPLR} = a6 \cdot PLR + b6$$

i_6 = coefficients listed in Appendix 4.0 EnergyPlus Modeling Coefficients (Table 27)

Comparison of the average measured power to the power calculated with the presented equations is in Figure 31.

Figure 31: Measured vs. Modeled Average Power, kW.

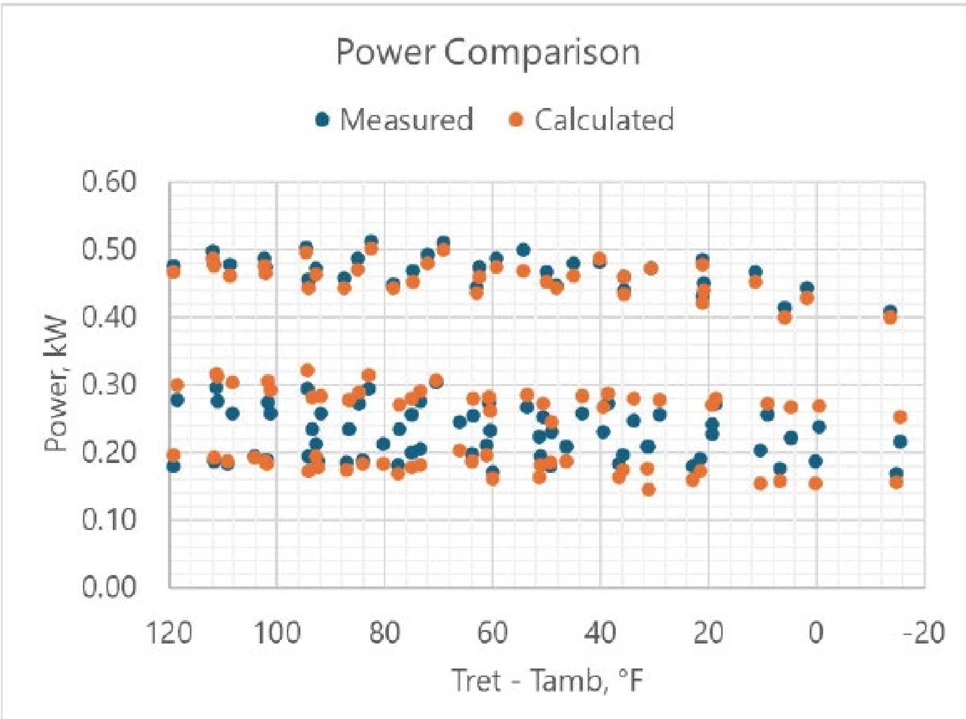

Modeling Strategy Accuracy

The performance characterizations presented in EnergyPlus Performance Curve Development Section were used to model the GAHP 80K performance and compared with measured test data in the following section. Generally, the modeling accuracy is about ±5% at full load and about ±10% at lower part load ratios as shown in Figure 32 in the computation of the COP (gas-only).

Figure 32: Measured vs. Modeled Error.

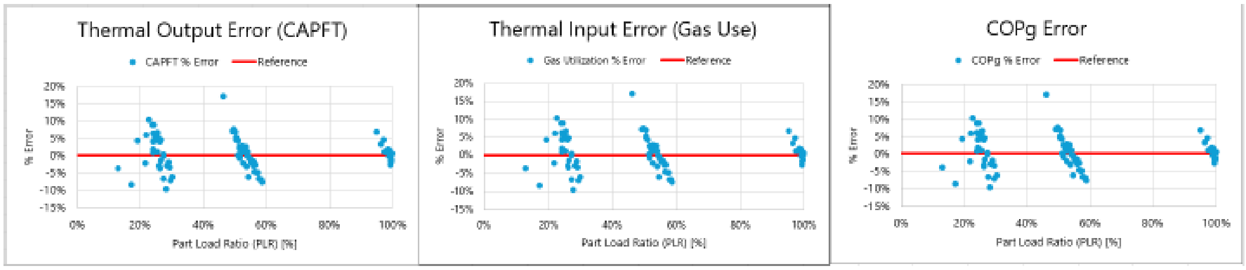

The EnergyPlus model includes a factor to account for the defrost performance penalty (up to 1.4% near 35°F). More extensive testing would be required to revise the modeling tool's default defrost performance curve. Until further testing is performed, the recommendation is to use the default defrost performance curve currently available in EnergyPlus.

Robur GAHP-A vs. ANESI GAHP 80K

This study follows a comprehensive study that was conducted on the Robur GAHP-A unit. The full report can be found on the California Emerging Technologies Program (ETP) Portal under the project ET23SWG0015. The most notable findings will be included in this report to compare GAHP manufacturer's performances.

Steady State Results

The Robur GAHP-A COP (gas only) and the ANESI GAHP 80K COP (gas only) performance curves as a function of the normalizing factor (RT-OAT) are included in Figure 33. Note that due to control algorithm differences between the Robur GAHP-A and ANESI GAHP 80K, the Robur GAHP-A is configured to operate according to the propylene glycol/water mixture flowrate which may prompt short cycling if operations are not configured according to the application. The ANESI GAHP 80K unit was configured to operate based off variability in the magnitude of the firing rate to avoid unwanted short cycling behavior. Nonetheless, on average, the COP (gas only) shows negligible differences at the higher RT-OATs. However, at lower RT-OATs, beginning at approximately 80°F, the Robur GAHP A's COP (gas only) drops slightly more than the ANESI GAHP 80K's COP (gas only) by approximately 0.2.

Figure 33: Robur GAHP-A vs. ANESI GAHP 80K COP (gas only) Steady State Performance.

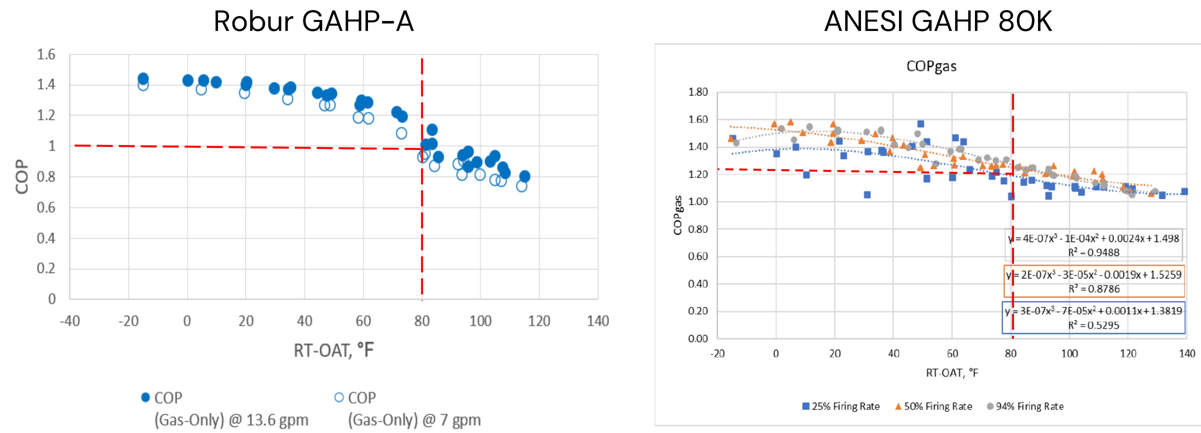

Load Based Results

The Robur GAHP-A COP (gas only) ratio and the ANESI GAHP 80K COP (gas only) ratio performance curves as a function of the PLR are included in Figure 34. On average, the differences in the part load performance between the Robur GAHP-A and ANESI GAHP 80K units are negligible and are independent of flowrate (Robur GAHP-A) or firing rate (ANESI GAHP 80K).

Figure 34: Robur GAHP-A vs. ANESI GAHP 80K COP (gas only) Load Based Performance.

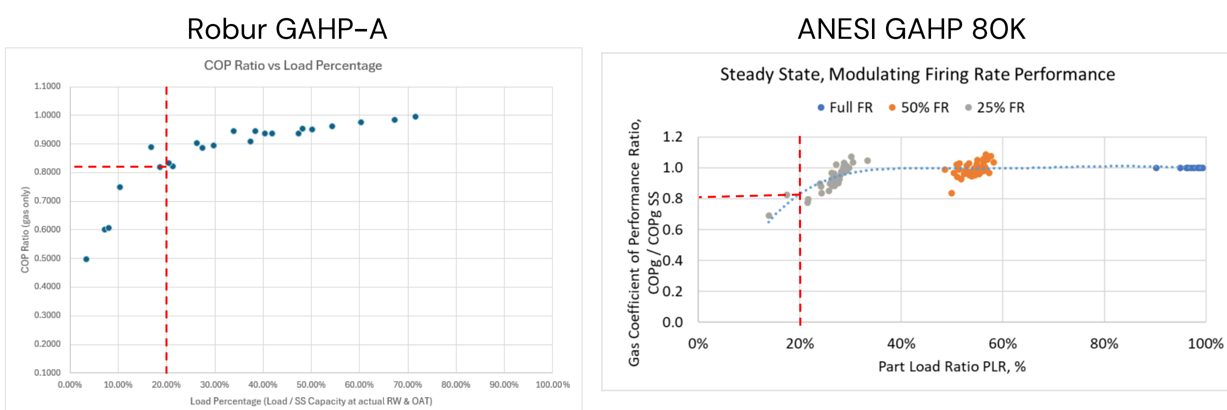

EnergyPlus Modeling Results

Table 14 includes a summary of the primary modeled parameters for both the Robur GAHP-A and ANESI GAHP 80K units. The differences in percent error are negligible, therefore, signifying that sufficient performance mapping laboratory data was extracted from both manufacturer's test matrices.

Table 14: Robur GAHP-A vs. ANESI GAHP 80K COP (gas only) Measure vs. Modeled Data % Error.

Variable	Robur GAHP-A % Error	ANESI GAHP 80K % Error
Thermal Output	±5%	±5% (at full load) ±10% (at lower PLRs)
Thermal Input		
COP (gas only)	±6%	

Conclusions

A comprehensive test matrix was established to gain a thorough understanding of how the GAHP 80K unit operates under various steady state and load-based conditions. The key independent variables across both tests were the OAT, firing rate, RT, tank setpoint, and draw rate.

For the steady state testing conditions:

1) The GAHP performed to expectations from the manufacturer's rated conditions-actual performance will modulate the firing rate. At standard conditions (47°F OAT, 95°F RT) the published COP is 1.43 with the testing result COP at 1.46.
2) At the most common operating points (RT-OAT of 60-80°F), the unit operated at $COP_{gas+electric}$ of 1.2-1.3, over the entire firing range. This demonstrates the energy savings potential of the unit for actual installations.
3) Cycling behavior noted at 140°F RT and 25% firing rate is expected at the operating limits of the GAHP. The GAHP continued to control the hydronic temperature through the cycles. With a storage tank to buffer any temperature variation, the end user would not be impacted.
4) Defrost characterization is very dependent on test conditions. A humidifier was ducted into the environmental chamber and directed towards the GAHP coil. Operating at maximum relative humidity that could be achieved in the test setup, there were about 16 hours between defrost cycles, and each cycle duration was approximately 26 minutes. The small duration relative to the time between cycles negated most impact on COP determined as an average over the time between defrost cycles.

For the load-based testing conditions:

1) The GAHP system performance is linearly related to the part load ratio, ranging from 90-100% over the part load range of 20-100%. This demonstrates minimal reduction in performance over a broad operating range.
2) Tank losses for the GAHP system test reduced COP by approximately 5%. Interconnecting piping losses were approximately 15% but are not representative of field installs due to length and level of insulation.

3) During load-based tests, the GAHP controls strategy did not utilize reduced firing as much as expected. For example, during standby tests when reduced firing would be expected, the heating calls were satisfied with the unit firing at 100%. Draw pattern tests showed that unit operated at 100% firing rate until the ST approached 140°F (maximum supply limitation).
4) During the draw pattern tests, fluctuating RTs from the indirect storage tank resulted in non-steady operation of the GAHP despite high loads and run times. The performance of the unit relative to steady state was reduced by less than 10%.
5) Fluctuating RTs from the indirect storage tank from the intermittent draw pattern resulted in non-steady operation of the GAHP despite high loads and extended run times. Performance relative to steady state was affected slightly over the 20-100% part load ratio. It is believed that firmware updates tested on the replacement unit played a significant role, highlighting the importance of effective control algorithms to achieve high efficiency.
6) Overall system performance improvement may be possible through integration of the indirect tank with an external heat exchanger. In addition, modified control strategies allowing the GAHP to control operation based on different tank temperatures rather than the aquastat could lead to performance improvements.

Close alignment of the model prediction data to the measured data of about ±5% accuracy at full load and ±10% accuracy at lower part load ratios provides sufficient confirmation for integration of the GAHP 80K laboratory data into EnergyPlus. The load-based testing represents the system model. Therefore, this may result in relatively higher error margins since the system parameters are specific to each configuration tested (i.e., tank size, heat exchanger effectiveness, controls strategy). An in-depth system parameter test matrix is beyond the scope of this study, therefore, the analysis is performed at a system level.

Recommendations

This study provided the following recommendations based on the laboratory study and EnergyPlus performance curve development:

1) Additional experimental defrost testing with the GAHP 80K unit should be conducted to provide additional input on the default defrost performance curve currently in EnergyPlus.
2) Overall system enhancements (i.e., varying heat exchanger configurations, more temperature sensors, and the inclusion of a tankless water heater) as previously described should be explored to gain a comprehensive understanding of varying affects on the GAHP.
3) To further contribute to the EnergyPlus GAHP modeling portfolio, additional prototype and commercially available GAHP units should be tested. It is

recommended that a similar test plan as the GAHP 80K unit, where applicable, be developed to draw comparison conclusions related to the parameters analyzed in this study.

4) Field testing should be conducted to simulate actual conditions and further provide insight into how the system operates and how it should be modeled.
5) To gain additional insights into the GAHP 80K operability and resultant emissions, it is recommended to conduct hydrogen blend testing up to 30%.

Appendices

Appendix 1.0 Test Rig Setup

Testbed Hydronic Test Rig

The ANESI GAHP 80K unit was plumbed to the THP testbed hydronic test rig and filled with propylene glycol. The propylene glycol percentage in the heat recovery fluid was 37% with deviations in density and specific heat from water, as shown in Table 15. These 37% propylene glycol water mix properties were using the resulting energy input and output calculations to be discussed in the Results subsection of the Equipment Commissioning section.

Table 15: Fluid Properties.

Temperature, °F	Density, lbm/cF			Specific Heat, Btu/lbm-°F		
	Water	PG @ 37%	% Diff.	Water	PG @ 37%	% Diff.
40	8.34	8.89	6.54%	1.000	0.895	-10.34%
60	8.33	8.82	5.87%	0.998	0.916	-8.21%
80	8.31	8.76	5.36%	0.998	0.934	-6.40%
100	8.29	8.70	4.89%	0.998	0.949	-4.87%
120	8.25	8.64	4.71%	0.999	0.962	-3.74%
140	8.21	8.59	4.57%	1.001	0.971	-2.99%
PG = propylene glycol						
Diff. = difference						

Gas Valve Set-Up

Prior to testing, the gas valve was adjusted to account for site-specific conditions before the initial test period, following guidelines in the ANESI GAHP 80K Installation Manual [4]. By default, the ANESI GAHP 80K is factory set to for slightly rich combustion. Figure 35 shows the setup and gas analyzer output at 30% burner demand.

Figure 35: Exhaust Gas Constituent Measurements.

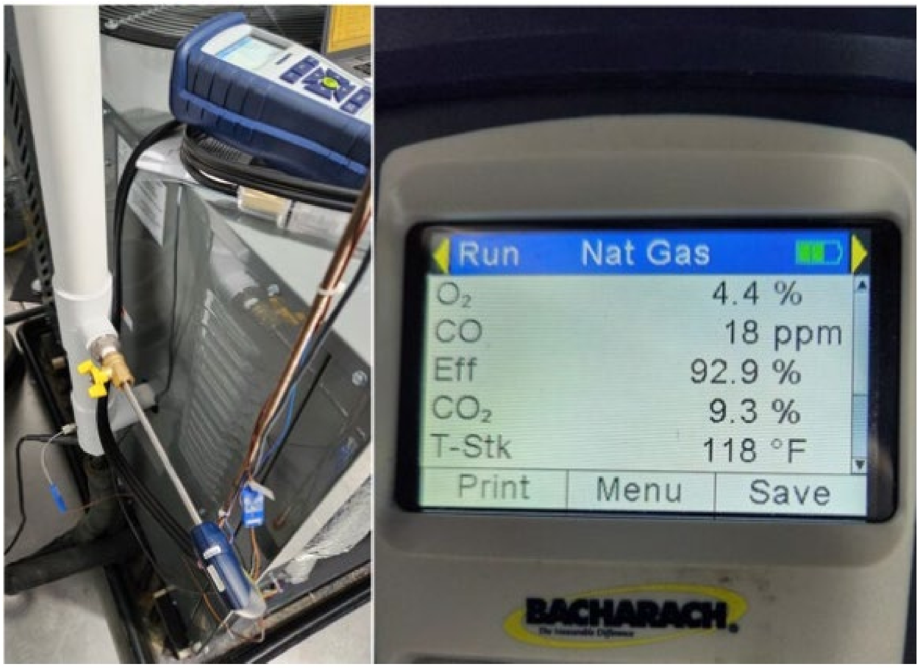

Table 16 shows the resulting oxygen (O_2), carbon dioxide (CO_2), gas flow, and firing rate at the set burner demand based on the building gas supply high-heating value (HHV) 1,050 BTU/cu ft. It should be noted that the ANESI GAHP 80K instructions assume the technician performing the installation will know the gas input HHV. The HHV is variable, and it is likely that the technician will not know the particular value at the time of installation, so the firing rate in actual practice could vary significantly.

Table 16: Gas Valve Adjustment Tests.

Burner Demand, %	Exhaust Gas O_2, %	Exhaust Gas CO_2, %	Measured Gas Flow, cfh	Firing Rate, Btu/h
30	4.4	9.3	18.7	19,800
90	4.4	9.3	52.5	55,400

Appendix 2.0 Steady State Results

Table 17: Steady-State Results Summary – Low Firing Rate (25%).

Target Conditions			Test Results, 15-min average				Cycling Rates and Performance			
Outside	Flow	Return	Outside	Flow	Return	Heating	Thermal	Power,	COP	COP
0	8.5	95	0.6	8.10	94.7	18.51	16.67	0.19	1.11	1.07
0	8.5	110	0.3	8.46	109.5	18.56	16.68	0.18	1.11	1.07
0	8.5	120	0.3	8.52	119.4	18.44	16.59	0.18	1.11	1.07
0	8.5	140	-0.4	8.16	138.9	18.83	17.53	0.19	1.07	1.04
7	8.5	95	7.7	8.37	94.7	19.17	16.59	0.18	1.16	1.11
7	8.5	110	7.6	8.48	109.5	18.29	16.47	0.19	1.11	1.07
7	8.5	120	7.6	8.21	119.4	18.12	16.29	0.19	1.11	1.07
7	8.5	140	7.4	8.15	138.9	18.02	17.19	0.19	1.05	1.01
17	8.5	95	17.3	8.37	95.0	18.71	16.24	0.18	1.15	1.11
17	8.5	110	17.4	8.46	109.7	17.80	15.87	0.19	1.12	1.08
17	8.5	120	17.5	8.51	119.6	17.46	15.92	0.19	1.10	1.05
17	8.5	140	17.5	8.57	139.1	18.15	16.57	0.20	1.09	1.05
35	8.5	95	34.8	7.87	95.0	18.27	15.49	0.17	1.18	1.14
35	8.5	110	34.8	8.44	109.9	18.67	15.39	0.20	1.21	1.16
35	8.5	120	35.4	8.54	119.6	17.27	15.11	0.19	1.14	1.10
35	8.5	140	35.3	8.46	139.4	14.87	13.91	0.19	1.07	1.02
47	8.5	95	45.9	8.39	95.3	23.93	15.26	0.18	1.57	1.51
47	8.5	110	46.0	8.48	110.1	20.94	14.57	0.20	1.44	1.37
47	8.5	120	46.4	8.54	119.9	17.32	14.56	0.20	1.19	1.14
47	8.5	140	46.6	8.62	139.5	15.20	14.58	0.21	1.04	0.99
60	8.5	95	59.0	8.39	95.5	19.47	14.30	0.18	1.36	1.30
60	8.5	110	58.9	8.48	110.1	20.24	14.05	0.19	1.44	1.38
60	8.5	120	58.9	8.54	120.0	20.35	13.87	0.21	1.47	1.40
60	8.5	140	59.3	8.62	139.5	13.78	13.25	0.21	1.04	0.99
75	8.5	95	72.6	8.39	95.5	18.87	14.12	0.18	1.34	1.28
75	8.5	110	74.3	8.49	110.3	19.25	14.01	0.20	1.37	1.31
75	8.5	120	73.8	8.54	120.2	19.46	13.87	0.21	1.40	1.33
75	8.5	140	73.7	8.60	139.8	16.95	13.73	0.24	1.23	1.16
90	8.5	95	89.2	8.40	95.9	18.60	13.30	0.18	1.40	1.34
90	8.5	110	89.1	8.49	110.7	19.33	13.38	0.19	1.44	1.38
90	8.5	120	89.0	8.54	120.3	17.83	13.02	0.21	1.37	1.30
90	8.5	140	88.6	8.61	140.0	11.38	9.72	0.22	1.17	1.09
110	8.5	95	110.8	8.37	96.0	17.51	11.98	0.17	1.46	1.39
110	8.5	110	110.7	8.47	110.9	15.95	11.82	0.19	1.35	1.28
110	8.5	120	110.2	8.53	120.6	14.26	11.94	0.20	1.19	1.13
110	8.5	140	109.1	8.61	140.2	9.06	8.59	0.21	1.05	0.97

Table 18: Steady-State Results Summary – Mid Firing Rate (50%).

Target Conditions			Test Results, 15-min average					Cycling Rates and Performance		
Outside Air Temp, °F	Flow Rate, gpm	Return Temp., °F	Outside Air Temp., °F	Flow Rate, gpm	Return Temp., °F	Heating Output, kBtu/h†	Thermal Input, kBtu/h†	Power, kW†	COP (Gas-Only)	COP (Gas + Electric)
0	8.5	95	0.9	8.40	94.4	40.56	33.42	0.23	1.21	1.19
0	8.5	110	0.9	8.50	109.2	39.98	32.74	0.26	1.22	1.19
0	8.5	120	0.6	8.55	119.1	36.27	32.75	0.28	1.11	1.08
0	8.5	140	0.7	8.59	128.6	34.38	32.38	0.30	1.06	1.03
7	8.5	95	7.8	8.42	94.3	41.05	32.79	0.23	1.25	1.22
7	8.5	110	7.8	8.51	109.2	38.66	32.52	0.26	1.19	1.16
7	8.5	120	7.9	8.57	119.0	38.77	32.23	0.28	1.20	1.17
7	8.5	140	7.9	8.60	128.6	34.36	31.83	0.30	1.08	1.05
17	8.5	95	17.3	8.42	94.6	40.89	32.15	0.23	1.27	1.24
17	8.5	110	17.6	8.50	109.4	38.19	31.73	0.26	1.20	1.17
17	8.5	120	17.5	8.55	119.1	38.41	31.53	0.27	1.22	1.18
17	8.5	140	17.6	8.59	128.9	36.75	31.38	0.30	1.17	1.13
35	8.5	95	34.4	8.43	94.9	40.68	30.83	0.23	1.32	1.29
35	8.5	110	34.6	8.52	109.6	38.91	30.68	0.26	1.27	1.23
35	8.5	120	34.7	8.55	119.5	36.45	30.14	0.27	1.21	1.17
35	8.5	140	34.6	8.58	129.1	37.90	30.04	0.29	1.26	1.22
47	8.5	95	46.1	8.41	95.2	37.61	30.08	0.23	1.25	1.22
47	8.5	110	46.1	8.50	109.8	39.90	30.02	0.25	1.33	1.29
47	8.5	120	46.2	8.54	119.5	37.50	29.76	0.28	1.26	1.22
47	8.5	140	46.2	8.59	129.3	37.30	29.63	0.29	1.26	1.22
60	8.5	95	55.5	8.42	95.1	43.48	29.69	0.23	1.46	1.43
60	8.5	110	59.3	8.52	110.0	39.33	29.28	0.25	1.34	1.30
60	8.5	120	59.1	8.55	119.8	36.75	29.01	0.27	1.27	1.23
60	8.5	140	59.0	8.60	129.5	36.55	28.94	0.30	1.26	1.22
75	8.5	95	76.1	8.41	95.5	44.34	28.29	0.23	1.57	1.53
75	8.5	110	76.4	8.50	110.2	41.46	27.71	0.25	1.50	1.45
75	8.5	120	76.6	8.54	120.0	37.97	26.88	0.26	1.41	1.37
75	8.5	140	76.1	8.58	129.7	33.95	26.90	0.27	1.26	1.22
90	8.5	95	90.7	8.41	95.6	42.83	27.09	0.22	1.58	1.54
90	8.5	110	90.9	8.50	110.4	40.05	26.65	0.24	1.50	1.46
90	8.5	120	91.0	8.53	120.2	37.77	26.10	0.26	1.45	1.40
90	8.5	140	91.1	8.58	129.9	35.48	25.93	0.27	1.37	1.32
110	8.5	95	111.3	8.42	95.9	37.54	25.68	0.22	1.46	1.42
110	8.5	110	111.2	8.50	110.6	39.94	25.43	0.24	1.57	1.52
110	8.5	120	111.3	8.55	120.4	38.15	25.34	0.26	1.51	1.46
110	8.5	140	111.5	8.58	130.2	35.97	25.05	0.27	1.44	1.38

Table 19: Steady-State Results Summary – Full Firing Rate (100%).

Target Conditions			Test Results, 15-min average					Cycling Rates and Performance		
Outside Air Temp, °F	Flow Rate, gpm	Return Temp., °F	Outside Air Temp., °F	Flow Rate, gpm	Return Temp., °F	Heating Output, kBtu/h†	Thermal Input, kBtu/h†	Power, kW†	COP (Gas-Only)	COP (Gas + Electric)
0	8.5	95	0.4	8.39	94.7	72.55	60.72	0.45	1.19	1.17
0	8.5	110	0.5	8.49	109.4	68.55	60.30	0.48	1.14	1.11
0	8.5	120	0.0	8.52	119.1	64.17	59.47	0.48	1.08	1.05
0	8.5	140	-0.2	8.53	128.9	63.65	59.20	0.50	1.08	1.05
7	8.5	95	7.2	8.40	94.7	74.78	59.86	0.46	1.25	1.22
7	8.5	110	7.3	8.48	109.3	70.66	59.41	0.47	1.19	1.16
7	8.5	120	7.5	8.51	119.2	66.81	58.43	0.48	1.14	1.11
7	8.5	140	7.4	8.54	128.8	61.14	58.16	0.48	1.05	1.02
17	8.5	95	16.3	8.41	94.7	77.30	59.11	0.45	1.31	1.27
17	8.5	110	16.6	8.47	109.5	72.18	58.40	0.47	1.24	1.20
17	8.5	120	17.0	8.51	119.4	68.08	57.92	0.49	1.18	1.14
17	8.5	140	17.2	8.54	129.1	64.19	57.50	0.50	1.12	1.08
35	8.5	95	32.0	8.36	95.1	79.17	57.07	0.45	1.39	1.35
35	8.5	110	34.8	8.45	109.7	73.37	56.46	0.47	1.30	1.26
35	8.5	120	34.5	8.52	119.6	69.05	56.02	0.49	1.23	1.20
35	8.5	140	34.6	8.55	129.4	66.25	55.53	0.50	1.19	1.16
47	8.5	95	47.1	8.39	95.3	83.01	55.40	0.45	1.50	1.46
47	8.5	110	47.5	8.46	110.0	76.30	55.06	0.47	1.39	1.35
47	8.5	120	47.6	8.51	119.7	72.51	54.78	0.49	1.32	1.28
47	8.5	140	47.2	8.55	129.6	68.01	54.43	0.51	1.25	1.21
60	8.5	95	59.8	8.41	95.5	81.82	53.96	0.44	1.52	1.48
60	8.5	110	60.3	8.47	110.2	76.28	53.66	0.47	1.42	1.38
60	8.5	120	60.5	8.51	119.9	72.77	53.17	0.49	1.37	1.33
60	8.5	140	60.6	8.55	129.7	68.97	52.80	0.51	1.31	1.26
75	8.5	95	74.6	8.41	95.6	78.74	52.01	0.43	1.51	1.47
75	8.5	110	74.6	8.48	110.3	79.09	51.94	0.46	1.52	1.48
75	8.5	120	75.3	8.52	120.2	71.80	51.58	0.48	1.39	1.35
75	8.5	140	75.6	8.56	130.0	65.38	51.19	0.50	1.28	1.24
90	8.5	95	89.8	8.41	95.8	72.79	50.05	0.41	1.45	1.41
90	8.5	110	89.5	8.48	110.4	75.63	50.07	0.45	1.51	1.47
90	8.5	120	89.5	8.52	120.3	75.61	50.10	0.47	1.51	1.46
90	8.5	140	89.9	8.56	130.1	70.49	49.75	0.48	1.42	1.37
110	8.5	95	109.6	8.40	96.1	68.58	47.91	0.41	1.43	1.39
110	8.5	110	109.2	8.48	110.9	73.18	47.78	0.44	1.53	1.48
110	8.5	120	109.2	8.53	120.6	73.59	47.64	0.47	1.54	1.49
110	8.5	140	109.3	8.55	130.4	72.42	47.54	0.49	1.52	1.47

Appendix 3.0 Part Load Results

Table 20: Load Based Results Summary – Standby.

Target Conditions			Test Results, 15-min average				Cycling Rates and Performance			
Outside Air Temp, °F	Flow Rate, gpm	Aquastat Temp., °F	Outside Air Temp., °F	Flow Rate, gpm	Return Temp., °F	Heating Output, kBtu/h	Thermal Input, kBtu/h	Power, kW	COP g (Gas-Only)	COP (Gas + Electric)
17	8.5	120	18.78	8.64	98.30	1.56	1.59	0.04	0.98	0.91
47	8.5	120	48.29	8.18	107.3	0.94	0.92	0.02	1.02	0.95
90	8.5	120	88.59	8.63	110.9	0.93	0.99	0.02	0.95	0.89
17	8.5	140	19.16	9.06	117.8	3.37	3.73	0.06	0.90	0.86
47	8.5	140	42.60	10.86	119.2	2.16	2.35	0.03	0.92	0.88
90	8.5	140	91.71	8.80	120.1	3.01	2.43	0.03	1.24	1.18

Table 21: Load Based Results Summary – Low Flow.

Target Conditions					Test Results, 15-min average			Cycling Rates and Performance		
Outside Air Temp, °F	Flow Rate, gpm	Aquastat, °F	Outside Air Temp., °F	Flow Rate, gpm	Return Temp., °F	Heating Output, kBtu/h	Thermal Input, kBtu/h	Power, kW	COP (Gas-Only)	COP (Gas + Electric)
12 GPH Original GAHP (Data included for reference only; not included in final analysis)										
17	8.5	120	17.61	9.33	100.49	9.41	9.96	0.11	0.95	0.91
47	8.5	120	41.19	9.17	102.96	8.60	8.30	0.09	1.04	1.00
90	8.5	120	89.19	8.63	106.86	8.32	7.17	0.07	1.16	1.13
17	8.5	140	18.17	8.85	112.21	12.57	13.71	0.14	0.92	0.89
47	8.5	140	41.25	8.78	115.00	12.06	11.98	0.12	1.01	0.97
90	8.5	140	90.73	8.64	117.99	11.04	8.90	0.10	1.24	1.20
24 GPH Original GAHP (Data included for reference only; not included in final analysis)										
17	8.5	120	18.32	9.24	104.73	15.23	15.82	0.16	0.96	0.93
47	8.5	120	43.36	9.12	106.22	14.26	13.55	0.16	1.05	1.01
90	8.5	120	91.43	8.58	106.77	14.82	11.62	0.12	1.28	1.23
17	8.5	140	18.89	9.24	114.85	21.82	23.16	0.21	0.94	0.91
47	8.5	140	41.58	11.36	117.01	21.13	20.80	0.19	1.02	0.98
90	8.5	140	92.08	8.90	120.12	19.96	16.06	0.16	1.24	1.20
12 GPH Replacement GAHP										
47	8.5	120	47.9	8.8	101.54	9.27	7.36	0.07	1.26	1.22

Target Conditions			Test Results, 15-min average					Cycling Rates and Performance		
Outside Air Temp, °F	Flow Rate, gpm	Aquastat, °F	Outside Air Temp., °F	Flow Rate, gpm	Return Temp., °F	Heating Output, kBtu/h	Thermal Input, kBtu/h	Power, kW	COP (Gas-Only)	COP (Gas + Electric)
24 GPH Replacement GAHP										
47	8.5	120	46.3	8.9	104.66	16.10	12.59	0.12	1.28	1.24

Table 22: Load Based Results Summary – Draw Pattern.

Target Conditions			Test Results, 15-min average					Cycling Rates and Performance		
Outside Air Temp, °F	Flow Rate, gpm	Aquastat, °F	Outside Air Temp., °F	Flow Rate, gpm	Return Temp., °F	Heating Output, kBtu/h	Thermal Input, kBtu/h	Power, kW	COP (Gas-Only)	COP (Gas + Electric)
Average Full Day – Original GAHP (Data included for reference only; not included in final analysis)										
47	8.5	120	46.41	8.86	110.02	22.78	20.76	0.19	1.10	1.06
47	8.5	120	44.92	8.86	111.50	46.28	41.04	0.37	1.13	1.09
47	8.5	120	46.31	8.79	108.47	56.51	48.02	0.42	1.18	1.14
47	8.5	140	41.87	10.72	119.84	30.61	29.67	0.27	1.03	1.00
47	8.5	140	36.27	10.54	114.92	54.90	50.72	0.44	1.08	1.05
47	8.5	140	46.01	8.77	111.11	60.56	50.69	0.45	1.19	1.16
Average Full Day - Replacement GAHP										
47	8.5	120	47.02	8.88	107.53	27.77	21.63	0.19	1.28	1.25
47	8.5	120	45.61	8.91	107.60	54.77	40.72	0.35	1.35	1.31
47	8.5	120	37.9	8.87	103.65	67.63	48.89	0.41	1.38	1.34
47	8.5	140	52.53	8.98	124.30	34.32	26.87	0.29	1.28	1.23
47	8.5	140	48.24	8.96	115.05	61.70	45.93	0.42	1.34	1.30
47	8.5	140	46.60	8.92	108.53	69.34	50.49	0.44	1.37	1.33
Each GAHP Heating Cycle										
1000 GPD, 120°F Aquastat - Replacement GAHP										
47	8.5	120	46.49	8.99	123.74	54.34	39.71	0.39	1.37	1.32
47	8.5	120	46.96	8.77	99.95	8.47	6.99	0.07	1.21	1.17
47	8.5	120	46.37	8.90	107.67	39.73	30.15	0.26	1.32	1.28
47	8.5	120	46.13	8.90	109.18	47.60	36.39	0.32	1.31	1.27
47	8.5	120	46.29	8.89	106.72	30.94	23.59	0.21	1.31	1.27
47	8.5	120	48.17	8.88	105.22	21.41	17.43	0.16	1.23	1.19
47	8.5	120	47.50	8.86	104.56	21.22	17.64	0.16	1.20	1.17
47	8.5	120	46.14	8.88	106.49	27.84	22.00	0.20	1.27	1.23
47	8.5	120	47.16	8.88	108.69	33.62	26.57	0.24	1.27	1.23

Target Conditions					Test Results, 15-min average			Cycling Rates and Performance		
Outside Air Temp, °F	Flow Rate, gpm	Aquastat, °F	Outside Air Temp., °F	Flow Rate, gpm	Return Temp., °F	Heating Output, kBtu/h	Thermal Input, kBtu/h	Power, kW	COP (Gas-Only)	COP (Gas + Electric)
47	8.5	120	47.20	8.88	109.45	37.43	29.03	0.26	1.29	1.25
47	8.5	120	48.23	8.89	109.59	41.13	31.74	0.28	1.30	1.26
47	8.5	120	47.57	8.87	108.67	43.78	34.66	0.31	1.26	1.23
47	8.5	120	48.66	8.87	107.92	40.61	31.43	0.28	1.29	1.25
47	8.5	120	47.14	8.88	108.67	33.28	25.21	0.23	1.32	1.28
3000 GPD, 120°F Aquastat - Replacement GAHP										
47	8.5	120	46.21	8.93	108.95	67.38	51.85	0.45	1.30	1.26
47	8.5	120	46.73	8.88	103.90	15.96	12.52	0.12	1.27	1.24
47	8.5	120	45.88	8.85	104.79	19.21	15.01	0.14	1.28	1.24
47	8.5	120	46.10	8.89	105.97	71.39	52.62	0.44	1.36	1.32
47	8.5	120	45.38	8.91	108.73	57.93	43.49	0.37	1.33	1.29
47	8.5	120	45.78	8.91	108.24	48.58	36.80	0.32	1.32	1.28
47	8.5	120	41.06	8.90	108.17	49.46	38.93	0.33	1.27	1.23
47	8.5	120	45.41	8.88	108.11	48.79	37.90	0.33	1.29	1.25
47	8.5	120	46.75	8.87	108.27	48.41	37.68	0.33	1.28	1.25
47	8.5	120	44.38	8.92	109.17	70.16	51.95	0.44	1.35	1.31
47	8.5	120	46.55	8.90	109.32	37.90	29.99	0.27	1.26	1.23
47	8.5	120	57.15	8.87	105.37	15.70	12.23	0.12	1.28	1.24
47	8.5	120	48.91	8.89	105.14	19.09	14.32	0.13	1.33	1.29
47	8.5	120	45.02	8.93	105.28	73.69	53.22	0.44	1.38	1.35
47	8.5	120	46.04	8.94	108.78	61.07	45.64	0.39	1.34	1.30
47	8.5	120	46.40	8.91	109.15	50.13	37.77	0.33	1.33	1.29
47	8.5	120	45.14	8.90	108.50	50.35	38.35	0.34	1.31	1.27
47	8.5	120	45.76	8.90	108.49	50.59	38.47	0.34	1.32	1.28
47	8.5	120	45.82	8.90	108.58	50.86	38.71	0.34	1.31	1.28
47	8.5	120	45.38	8.94	108.45	71.42	52.04	0.44	1.37	1.33
5000 GPD, 120°F Aquastat - Replacement GAHP										
47	8.5	120	37.45	8.85	102.63	77.42	55.70	0.46	1.39	1.35
47	8.5	120	35.76	8.98	112.50	76.31	57.21	0.49	1.33	1.30
47	8.5	120	44.38	8.91	108.14	38.75	29.35	0.26	1.32	1.28
47	8.5	120	45.38	8.89	106.14	21.78	16.75	0.15	1.30	1.26
1000 GPD, 120°F Aquastat - Original GAHP (Data included for reference only; not included in final analysis)										
47	8.5	120	48.51	8.71	104.47	6.42	6.05	0.06	1.06	1.02
47	8.5	120	47.91	8.90	110.27	23.75	21.78	0.20	1.09	1.06
47	8.5	120	47.98	8.86	111.97	40.11	35.74	0.32	1.12	1.09

Target Conditions					Test Results, 15-min average			Cycling Rates and Performance		
Outside Air Temp, °F	Flow Rate, gpm	Aquastat, °F	Outside Air Temp., °F	Flow Rate, gpm	Return Temp., °F	Heating Output, kBtu/h	Thermal Input, kBtu/h	Power, kW	COP (Gas-Only)	COP (Gas + Electric)
47	8.5	120	47.69	8.85	110.99	43.59	38.57	0.35	1.13	1.10
47	8.5	120	48.27	9.03	109.56	29.49	27.72	0.25	1.06	1.03
47	8.5	120	47.58	8.86	109.57	22.38	20.28	0.19	1.10	1.07
47	8.5	120	47.64	8.95	106.95	15.37	14.08	0.13	1.09	1.06
47	8.5	120	47.50	8.83	108.47	21.77	19.48	0.18	1.12	1.08
47	8.5	120	47.07	8.98	109.75	23.06	21.11	0.20	1.09	1.06
47	8.5	120	47.03	8.98	111.35	30.51	28.09	0.26	1.09	1.05
47	8.5	120	47.29	8.83	111.63	33.96	31.02	0.29	1.09	1.06
47	8.5	120	46.98	8.78	111.86	35.67	32.66	0.30	1.09	1.06
47	8.5	120	46.97	8.95	111.63	34.03	31.76	0.29	1.07	1.04
47	8.5	120	47.14	8.95	108.55	19.68	18.09	0.17	1.09	1.05
47	8.5	120	45.76	8.76	106.25	9.54	8.93	0.09	1.07	1.03
47	8.5	120	47.35	8.94	111.99	45.64	39.78	0.36	1.15	1.11
47	8.5	120	46.94	8.88	111.69	43.97	39.11	0.35	1.12	1.09
47	8.5	120	46.72	8.79	110.99	28.03	25.69	0.24	1.09	1.06
47	8.5	120	45.79	9.03	108.99	23.78	21.75	0.20	1.09	1.06
47	8.5	120	45.81	8.83	107.18	16.29	14.91	0.14	1.09	1.06
47	8.5	120	44.95	8.73	108.55	21.90	19.90	0.18	1.10	1.07
47	8.5	120	46.48	8.73	109.91	23.43	21.48	0.20	1.09	1.06
47	8.5	120	45.94	9.02	111.07	30.98	28.43	0.26	1.09	1.06
47	8.5	120	46.04	8.91	111.95	34.16	31.12	0.29	1.10	1.06
47	8.5	120	46.58	8.69	111.65	35.54	32.42	0.30	1.10	1.06
47	8.5	120	46.24	8.94	111.35	34.15	31.00	0.29	1.10	1.07
47	8.5	120	44.57	8.83	108.32	19.92	18.43	0.17	1.08	1.05
47	8.5	120	44.72	8.94	106.72	9.77	9.13	0.09	1.07	1.03
47	8.5	120	46.33	8.83	112.24	46.59	41.31	0.37	1.13	1.09
47	8.5	120	45.91	8.70	110.21	40.35	36.43	0.33	1.11	1.07
47	8.5	120	46.34	8.65	110.71	30.84	28.50	0.27	1.08	1.05
47	8.5	120	44.25	9.09	108.52	23.75	21.60	0.20	1.10	1.07
47	8.5	120	44.89	8.84	107.22	16.35	15.19	0.14	1.08	1.04
47	8.5	120	43.47	8.84	108.23	21.74	19.92	0.18	1.09	1.06
47	8.5	120	45.27	9.08	110.03	25.01	23.03	0.21	1.09	1.05
47	8.5	120	45.76	8.80	111.64	31.79	28.96	0.27	1.10	1.06
47	8.5	120	46.04	8.70	111.80	33.61	30.68	0.28	1.10	1.06
47	8.5	120	45.80	8.77	111.70	36.05	32.91	0.30	1.10	1.06
47	8.5	120	46.10	8.86	111.28	33.61	30.87	0.29	1.09	1.06
47	8.5	120	44.38	8.92	110.27	28.40	25.98	0.24	1.09	1.06

Target Conditions			Test Results, 15-min average					Cycling Rates and Performance		
Outside Air Temp, °F	Flow Rate, gpm	Aquastat, °F	Outside Air Temp., °F	Flow Rate, gpm	Return Temp., °F	Heating Output, kBtu/h	Thermal Input, kBtu/h	Power, kW	COP (Gas-Only)	COP (Gas + Electric)
3000 GPD, 120°F Aquastat - Original GAHP (Data included for reference only; not included in final analysis)										
47	8.5	120	44.86	8.74	106.70	14.55	13.44	0.13	1.08	1.05
47	8.5	120	43.93	8.93	107.33	17.02	15.81	0.15	1.08	1.04
47	8.5	120	43.98	8.95	109.97	63.12	54.58	0.48	1.16	1.12
47	8.5	120	45.16	8.74	111.97	49.48	43.90	0.40	1.13	1.09
47	8.5	120	44.65	8.86	111.43	42.80	38.89	0.35	1.10	1.07
47	8.5	120	44.65	8.76	111.41	44.01	39.55	0.36	1.11	1.08
47	8.5	120	46.12	8.87	110.94	42.59	38.14	0.35	1.12	1.08
47	8.5	120	45.55	8.83	111.05	42.39	37.70	0.35	1.12	1.09
47	8.5	120	44.78	8.89	110.76	53.03	46.27	0.42	1.15	1.11
47	8.5	120	44.77	8.95	113.47	62.91	55.28	0.50	1.14	1.10
47	8.5	120	46.31	8.72	112.19	30.89	28.26	0.26	1.09	1.06
47	8.5	120	44.31	8.81	106.60	14.60	13.53	0.13	1.08	1.05
47	8.5	120	43.50	8.84	107.24	16.76	15.58	0.15	1.08	1.04
47	8.5	120	43.80	8.88	111.38	62.93	54.27	0.48	1.16	1.13
47	8.5	120	45.42	8.82	112.45	47.18	41.61	0.37	1.13	1.10
47	8.5	120	44.70	8.75	111.01	41.87	37.80	0.34	1.11	1.07
47	8.5	120	45.05	8.89	112.11	42.27	37.93	0.35	1.11	1.08
47	8.5	120	45.55	8.84	111.69	42.56	38.26	0.35	1.11	1.08
47	8.5	120	45.27	8.83	111.93	42.24	37.93	0.35	1.11	1.08
47	8.5	120	44.68	8.92	111.25	53.01	46.46	0.42	1.14	1.11
47	8.5	120	45.08	8.85	113.18	62.17	55.06	0.49	1.13	1.10
47	8.5	120	45.65	8.73	112.67	52.74	48.07	0.44	1.10	1.06
47	8.5	120	46.10	8.79	111.07	32.42	30.25	0.28	1.07	1.04
47	8.5	120	44.07	8.78	106.50	15.00	13.98	0.13	1.07	1.04
47	8.5	120	44.94	8.99	107.49	16.34	15.47	0.14	1.06	1.02
47	8.5	120	44.82	8.89	110.98	62.03	54.37	0.48	1.14	1.11
47	8.5	120	46.16	8.89	112.72	46.76	41.65	0.37	1.12	1.09
47	8.5	120	46.04	8.74	111.19	41.81	37.67	0.34	1.11	1.08
47	8.5	120	46.34	8.76	112.04	41.59	37.65	0.34	1.10	1.07
47	8.5	120	46.39	8.95	111.34	41.99	37.90	0.35	1.11	1.07
47	8.5	120	46.03	8.87	111.40	41.40	37.62	0.34	1.10	1.07
47	8.5	120	45.78	8.78	111.71	50.98	45.99	0.41	1.11	1.08
47	8.5	120	45.35	8.84	113.79	63.23	54.93	0.49	1.15	1.12
5000 GPD, 120°F Aquastat - Original GAHP (Data included for reference only; not included in final analysis)										
47	8.5	120	46.47	8.81	107.94	23.55	21.90	0.20	1.08	1.04

Target Conditions					Test Results, 15-min average			Cycling Rates and Performance		
Outside Air Temp, °F	Flow Rate, gpm	Aquastat, °F	Outside Air Temp., °F	Flow Rate, gpm	Return Temp., °F	Heating Output, kBtu/h	Thermal Input, kBtu/h	Power, kW	COP (Gas-Only)	COP (Gas + Electric)
47	8.5	120	46.95	8.58	107.94	19.77	18.23	0.17	1.08	1.05
47	8.5	120	46.78	8.79	111.49	30.72	27.81	0.25	1.10	1.07
47	8.5	120	45.53	8.67	107.52	65.66	55.65	0.49	1.18	1.15
47	8.5	120	46.32	8.70	109.36	65.64	55.51	0.48	1.18	1.15
47	8.5	120	47.29	8.96	111.31	46.23	41.20	0.37	1.12	1.09
47	8.5	120	47.12	9.07	106.54	15.74	14.43	0.14	1.09	1.06
47	8.5	120	47.53	8.86	110.34	27.35	25.34	0.23	1.08	1.05
47	8.5	120	46.07	8.87	106.80	66.56	55.28	0.48	1.20	1.17
47	8.5	120	47.33	8.98	111.84	58.45	51.61	0.46	1.13	1.10
47	8.5	120	46.64	8.87	108.65	66.33	55.21	0.48	1.20	1.17
1000 GPD, 140°F Aquastat - Original GAHP (Data included for reference only; not included in final analysis)										
47	8.5	140	41.76	9.43	117.04	14.26	13.78	0.13	1.03	1.00
47	8.5	140	39.24	11.37	118.58	52.21	48.76	0.43	1.07	1.04
47	8.5	140	41.25	11.16	118.90	26.95	26.40	0.24	1.02	0.99
47	8.5	140	41.40	11.61	118.12	24.71	24.52	0.23	1.01	0.98
47	8.5	140	42.34	11.33	120.56	34.98	33.76	0.31	1.04	1.00
47	8.5	140	43.85	11.57	121.80	39.84	39.58	0.36	1.01	0.98
47	8.5	140	43.89	9.01	121.38	45.31	44.08	0.40	1.03	1.00
47	8.5	140	43.35	10.72	118.93	23.90	24.51	0.23	0.98	0.95
47	8.5	140	40.14	11.04	118.03	30.06	28.68	0.26	1.05	1.02
47	8.5	140	41.55	11.02	119.07	26.79	26.64	0.25	1.01	0.97
47	8.5	140	42.64	10.73	118.17	24.67	24.81	0.23	0.99	0.96
47	8.5	140	43.29	11.32	120.38	34.51	34.11	0.31	1.01	0.98
47	8.5	140	42.94	10.88	121.73	40.53	39.48	0.36	1.03	1.00
47	8.5	140	43.55	9.04	121.79	46.41	45.23	0.41	1.03	1.00
47	8.5	140	43.64	10.45	118.94	19.57	19.45	0.18	1.01	0.97
3000 GPD, 140°F Aquastat - Original GAHP (Data included for reference only; not included in final analysis)										
47	8.5	140	43.08	11.32	115.52	17.77	18.36	0.17	0.97	0.94
47	8.5	140	34.83	11.27	113.51	61.46	56.37	0.48	1.09	1.06
47	8.5	140	37.76	11.58	124.01	56.75	54.99	0.50	1.03	1.00
47	8.5	140	41.52	11.27	116.46	20.20	20.42	0.19	0.99	0.96
47	8.5	140	35.98	11.25	114.10	59.62	54.72	0.47	1.09	1.06
47	8.5	140	36.60	11.79	122.84	57.06	54.57	0.50	1.05	1.01
47	8.5	140	41.92	11.53	117.22	20.75	21.06	0.20	0.99	0.95
47	8.5	140	36.20	9.11	114.19	59.37	53.89	0.47	1.10	1.07

Target Conditions					Test Results, 15-min average			Cycling Rates and Performance		
Outside Air Temp, °F	Flow Rate, gpm	Aquastat, °F	Outside Air Temp., °F	Flow Rate, gpm	Return Temp., °F	Heating Output, kBtu/h	Thermal Input, kBtu/h	Power, kW	COP (Gas-Only)	COP (Gas + Electric)
5000 GPD, 140°F Aquastat - Original GAHP (Data included for reference only; not included in final analysis)										
47	8.5	140	48.10	8.87	120.99	28.09	26.73	0.25	1.05	1.02
47	8.5	140	44.73	8.90	108.84	67.58	55.43	0.49	1.22	1.18
47	8.5	140	47.00	8.93	123.77	57.15	51.40	0.49	1.11	1.08
47	8.5	140	47.35	8.76	109.88	17.31	16.10	0.15	1.07	1.04
47	8.5	140	45.56	8.67	109.55	67.20	55.34	0.49	1.21	1.18
47	8.5	140	47.10	8.66	119.14	61.12	53.37	0.49	1.15	1.11
47	8.5	140	48.53	8.82	120.63	26.14	24.52	0.24	1.07	1.03
47	8.5	140	46.63	8.69	108.74	65.53	53.87	0.47	1.22	1.18

*Individual cycle data not available for replacement GAHP with 140°F aquastat setpoint due to continuous operation.

Appendix 4.0 EnergyPlus Modeling Coefficients

Table 23: CAPFT Coefficients (Equation 9).

Coefficients	Values
a1	-1.200E+00
b1	6.410E-02
c1	-6.940E-03
d1	-6.291E-04
e1	2.852E-04
f1	-1.794E-04
g1	1.935E-06
h1	-1.724E-06
i1	1.368E-06
j1	1.982E-08

Table 24: EIRFT Coefficients (Equation 11).

Coefficients	Values
a2	8.003E-01
b2	-1.612E-02
c2	1.831E-04
d2	4.772E-03
e2	8.898E-05
f2	-1.380E-06

Table 25: EIRFPLR Coefficients (Equation 12).

Coefficients	Values
a3	-2.332E-02
b3	1.022E+00

Table 26: CRF Coefficients (Equation 15).

Coefficients	Values
a4	7.099E-01
b4	2.838E-01

Table 27: $Aux_{Elec,EIRFT}$ Coefficients (Equation 17).

Coefficienst	Values
a5	7.785E-01
b5	-2.173E-03
c5	-1.886E-05
d5	5.026E-08
e5	2.496E-03
f5	2.704E-05

Table 28: $Aux_{Elec,EIRFPLR}$ Coefficients (Equation 18).

Coefficients	Values
a6	1.155E+00
b6	6.754E-02

References

1. Guada, Alejandro; Van Dixhorn, Lee; Fridlyand, Alex; Katz, Ari. “Robur GAHP A Performance Mapping.” GTI Energy, 2023.
2. Talebi, Madeline; Long, Steven. “ET23SWG0015: Gas Absorption Heat Pump (GAHP) #1 Performance Mapping.” ICF – SCG Gas Emerging Technologies (GET) Program, 2024.
3. Ecotope. “Ecosizer – Central Heat Pump Water Heating Sizing Tool” (2025). *Ecotope*, https://ecosizer.ecotope.com/static/pdfs/ecosizer-chpwh-sizing-tool-manual07222024.pdf
4. Stone Mountain Technologies Institute (SMTI). “Installation and Operation Manual – Gas-Fired Air to Water Absorption Heat Pump.” *ANESI,* https://stonemountaintechnologies.com/wp-content/uploads/2024/01/Anesi-GAHP-80K-Installation-Operation-Manual-1123.pdf
5. Martin, Cara; Oppenheim, Paul; Bush, Josh; Stillman, Hal. “Alternative Defrost Strategies for Residential Heat Pumps” (2018). *International Refrigeration and Air Conditioning Conference*, https://www.ots-rd.com/wp-content/uploads/2023/09/Alternative_Defrost_Strategies_for_Residential_Heat_Pumps.pdf
6. “Technical Data Book” (2017). *Mitsubishi Electric*, https://meus1.mylinkdrive.com/viewPdf?srcUrl=http://s3.amazonaws.com/enter.mehvac.com/DAMRoot/Original/10003%5C2017_P-Series_Engineering_Manual.pdf
7. Fridlyand, Alex; Glanville, Paul; and Garrabrant, Michael, "Pathways to Decarbonization of Residential Heating" (2021). International High Performance Buildings Conference. Paper 354. https://docs.lib.purdue.edu/ihpbc/354
8. Van Dixhorn, Lee; Katz, Ari. “ANESI GAHP Performance Mapping.” GTI Energy, 2025.
9. 3 Superstor SSU-119-CN, https://www.htproducts.com/superstor-ultra-waterheater.html